INVESTIGATION OF RADIOWAVE PROPAGATION IMPAIRMENTS AT SUPER HIGH FREQUENCY DUE TO RAIN IN AKURE

BY

OLUWADARE, ESHOLOMO JOHN

PHY/97/9563

A THESIS SUBMITTED TO THE DEPARTMENT OF PHYSICS, SCHOOL OF SCIENCES, FEDERAL UNIVERSITY OF TECHNOLOGY, AKURE, NIGERIA.

IN PARTIAL FULFILMENT OF THE REQUIREMENT FOR THE AWARD OF A DEGREE OF MASTER OF TECHNOLOGY (M.Tech) IN COMMUNICATION PHYSICS.

DECEMBER, 2010

CERTIFICATION

Certification by the Student.

This work has not been presented elsewhere for the award of a degree, or any other purpose.

Candidate's Name: OLUWADARE, Esolomo. John.

Signature..... Date.20/12/2010

Certification by the Supervisors.

We hereby certify that this research work was carried out by Oluwadare Esolomo John, in the Department of Physics, Federal University of Technology, Akure under our joint supervision.

..... 20/12/2010

Prof. M. O. Ajewole. Date

(Major Supervisor)

..... 20/12/2010

Dr. S. E. Falodun. Date

(Co-Supervisor)

..... 20/12/2010

Dr. J.S. Ojo. Date

(Co-Supervisor)

..... 20/12/10

Prof. (Mrs.) I. A. Fuwape Date

Head of Department

DEDICATION

This work is dedicated to the memory of my father; Late Mr Moses Bello Oluwadare.

ACKNOWLEDGEMENTS

My profound gratitude goes to my supervisor, Prof. M. O. Ajewole for supervising this work. His effort and guidance towards the successful completion of this project are highly appreciated. May God the Almighty in His infinite mercy grant him and his family long life and prosperity (Amen).

I gratefully acknowledge the donation of the Micro Rain Radar used for this project by Alexander von Humboldt (AvH) Foundation and the University of Bonn Germany.

My special thanks also go to Dr. S.E. Falodun, Dr. J.S. Ojo, Dr. A.T. Adediji, Dr. A.B. Rabiu, Dr. E.O. Ogolo, Prof (Mrs.) I.A. Fuwape and all my lecturers for their encouragement, support and contribution to the success of this project. May God be with them all, (Amen). My appreciation also goes to all members of the Oluwadare's family. I commend the support and unfading love of my colleagues and dear ones, Awotuse Olamitomi, Samuel Okereke, Alao Olumuyiwa, Tomiwa Akinyemi among others. I am indeed indebted to my dear friend, Awotuse, for her invaluable assistance and scholarly guidance during my project. May she live long and prosper. I am equally grateful to Pastor David Omolafe and family for their support and understanding.

Finally, I am sincerely grateful to God Almighty for His love and mercy endures forever. Glory is to God. Amen.

TABLE OF CONTENTS

CHAPTER THREE

PROJECT SITE, INSTRUMENTATION AND METHODOLOGY

CHAPTER FOUR

RESULTS AND DISCUSSION

CHAPTER FIVE

CONCLUSIONS AND RECOMMENDATIONS

REFERENCES

LIST OF FIGURES

LIST OF TABLES

ABSTRACT

The measurement of the vertical profiles of rainfall parameters such as drop size distribution, rain rate, liquid water content, fall velocity and radar reflectivity were carried out by using Micro Rain Radar in 2006 and 2008 at Akure (Lat 5°15'E, long 7°15'N) in South-Western Nigeria. The vertical distributions of these parameters with heights are presented for 0 - 4800 m. The range gates for the measurement are 30 with a height step of 160 m. The variation of the drop size distribution, rain rate and liquid water content with height were evaluated. The highest rain rate and liquid water content were observed within the height range 0-160 m. For the all cases considered, the largest concentration of drop size with a diameter of 0.246 mm occurred in the height range 0-160 m. Empirical relations in the form $Y = aR^b$ have been obtained for the rainfall rate, the radar reflectivity factor Z, and liquid water content using the least square power law regression. The results show that the relationship obtained for height range 0-160 m for the two years were in good agreement with the values available in the literatures. For all cases considered, there is a good correlation between the parameters. The measured rainfall rates were divided into classes using the same criteria as described in Joss et at (1968) for stratiform rain type, rain rate R < 50mm/h and convective rain type, rain rate R > 50 mm/h. These empirical relations were compared with results obtained at other locations. Though there is a good agreement between the relationships Z-R in stratiform rain type with those in the literatures, however there is a slight difference with that of convective rain type. These parameters are then used to calculate specific attenuation due to rain at different rain types and rain rates. The specific attenuation was then evaluated for frequencies from 1 – 100 GHz. Results obtained show that specific attenuation increases with increasing frequency for both rain types; at a critical frequency (around 31 GHz), the increasing specific attenuation starts to decrease.

CHAPTER ONE

1.0 INTRODUCTION

Accurate measurement and prediction of the spatial and temporal distribution of rainfall are basic issues in communication. The measurement of various rainfall parameters have been carried out by many researchers using different instruments such as the rain gauge, used in the measurement of rain rate, and the disdrometer, used for drop size distribution measurement. With a known relationship, others parameters such as reflectivity and liquid water content are calculated from other measured parameters.

As a result of the gradual development of radar technology over the last 50 years, ground-based weather radar is now finally becoming a tool for quantitative measurement of rainfall parameters instead of merely using it for qualitative rainfall estimation.

Potential areas of application of ground-based weather radar systems in operational hydrology include storm hazard assessment and flood forecasting, warning, and control (Collier, 1989).

The term propagation is used to describe the transfer of energy without necessarily transferring matter. The transfer of energy between two points in certain media is a result of changes with time in the spatial distribution of the non-static field in that medium (this could be the electric or magnetic or both) but must change with time. The propagation medium has a great influence on the success of any telecommunication system. The International Telecommunication Union (ITU) has limited the term radio wave to electromagnetic waves with frequencies lower than 3000 GHz (Hall, 1991).

The concept of frequency is the key to the understanding of radio frequency because almost everything in the radio frequency world is frequency dependent. A signal is distinguished on the basis of its frequency. The range of frequencies used is also the most common way to

distinguish a wave from another. This is achieved by using the concept of frequency bands, i.e. the standard way to name specific range of frequencies. The list of radio frequency bands of common use to radio wave propagation is shown in Table 1.1

This study deals with the analysis of rainfall parameters measured by the vertically looking micro rain radar. The parameters measured include the drop size distributions, rain rate, liquid water content, fall velocity and the radar reflectivity factor. Some of these parameters are then used to calculate the attenuation due to rain when radio signal passes through the measured rain types. The frequency range of interest is from 3 GHz to 100 GHz. For the calculation of attenuation due to different rain types, the power law relationship between attenuation and rain rate as recommended by International Telecommunication Union were used with the power law constant "a" and "b" for frequencies of 3 - 100 GHz calculated using regression analysis developed by Ajewole et al., (1999) for Nigeria.

1.1 OBJECTIVES OF THE RESEARCH:

The specific objectives of the present work are to:

a. measure the vertical distribution of rainfall parameters (rain drop - size distributions, radar reflectivity, rain rate and liquid water content);

b. use the data obtained to validate the hitherto theoretically obtained power law constants of radar reflectivity, rain rate and liquid water content and rain rate and;

c. compute the specific attenuation due to rain at microwave frequencies.

1.2 MOTIVATION FOR THE STUDY

There have been extensive works done on the measurement of rain drop size distributions, radar reflectivity and rain rate for the investigation of rain-induced impairment to radio signals at super high frequencies. Table 1.1 shows the radiofrequency spectrum and their applications. Most of these works were carried out in the temperate regions. However, some researchers have carried out similar studies in tropical locations. Such studies include the measurement of rain drop size distributions at Ile-Ife by Ajayi and Olsen (1985), Adimula and Ajayi (1996) at Ilorin, Zaria and Calabar using the disdrometer, while the measurement of rainfall intensity was done by a rain gauge.

Until the present study, there has not been any measurement of the vertical profile of rainfall parameters in Nigeria. Previous measurements of the drop size distributions were done using the disdrometer usually placed at the ground level. Therefore, the uniqueness of this study is in using micro - rain radar, to measure the vertical profile of the drop size distributions, rain rate, liquid water content, fall velocity and the radar reflectivity factor simultaneously during a rain event.

Table 1.1: Radio frequencies and their applications.

Name	Designation	Frequency band	Wavelength	Applications
Extremely low frequency	ELF	3-30 Hz	10,000-100,000 km	Directly audible when converted to sound, communication with submarines
Super low frequency	SLF	30-300 Hz	1,000-10,000 km	Directly audible when converted to sound, AC power grids (50-60 Hz)
Ultra low frequency	ULF	300-3000 Hz	100-1,000 km	Directly audible when converted to sound, communication with mines
Very low frequency	VLF	3-30 kHz	10-100 km	Directly audible when converted to sound (ultrasound)
Low frequency	LF	30-300 kHz	1-10 km	AM broadcasting, navigation beacons
Medium frequency	MF	300-3000 kHz	100-1000 m	AM broadcasting, navigation beacons, maritime and aviation communication
High frequency	HF	3-30 MHz	10-100 m	Shortwave, amateur radio, citizens' band radio
Very high frequency	VHF	30-300 MHz	1-10 m	FM broadcasting, amateur radio, broadcast television, aviation, GPR
Ultra high frequency	UHF	300-3000 MHz	10-100 cm	Broadcast television, amateur radio, mobile telephones, cordless telephones, remote keyless entry for mobiles, GPR
Super high frequency	SHF	3-30 GHz	1-10 cm	Wireless networking, satellite links, satellite television, microwave links
Extremely high frequency	EHF	30-300 GHz	1-10 mm	Microwave data links, radio astronomy, remote sensing, advanced security scanning

CHAPTER TWO

LITERATURE REVIEW

2.1 WEATHER RADAR

A weather radar is used to locate precipitation, calculate its motion, estimate its type (rain, snow, hail and so on), and forecast its future position and intensity. Modern weather radars are mostly Doppler radars, which are capable of detecting the motion of rain droplets in addition to the intensity of the precipitation. Both types of data can be analyzed to determine the structure of storms and their potential to cause severe weather.

2.1.1 How Weather Radar Works

A radar beam spreads out as it moves away from the transmitter, covering an increasingly large volume. Weather radars send directional pulses of microwave radiation, of periods of about the order of a microsecond, using a cavity magnetron or klystron tube connected to a waveguide to a parabolic antenna. Rayleigh scattering occurs at frequencies where the rain drops size is within 2 mm. For wavelengths that are approximately ten times this size, part of the energy of each pulse will bounce off these small particles, and come back in the direction of the radar station. Shorter wavelengths are useful for smaller particles, but the signal is more quickly attenuated. Thus 10 cm (S-band) radar is preferred but is more expensive than a 5 cm C-band system. 3 cm X-band radar is used only for very short distance purposes, and 1 cm Ka-band weather radar is used only for research on small-particle phenomena such as drizzle and fog. Radar pulses spread out as they move away from the radar station. This means that the region of air any given pulse is moving through is larger for areas farther away from the station, and smaller for nearby areas, thereby decreasing resolution at far distances. At the end of a 150-200 km sounding range, the volume of air scanned by a single pulse

might be of the order of a cubic kilometer. The volume of air that a given pulse takes up at any point in time may be approximately calculated by the formula

$$v = hr^2\theta^2 \ (\mathrm{m}^3) \tag{2.1}$$

where v is the volume enclosed by the pulse, h is pulse width (metres), and calculated from the duration in seconds of the pulse times the speed of light, r is the distance from the radar that the pulse has already traveled (metres), and θ is the beam width (radians). This formula assumes that the beam is symmetrically circular; "r" is much greater than "h" so "r" taken at the beginning or at the end of the pulse is almost the same, and the shape of the volume is a cone frustum of depth "h".

2.1.2 Calibrating Intensity of Return

Since the targets are not unique in each volume, the radar equation has to be developed beyond the basic one:

$$P_r = \left[P_t \frac{G_t^2 \lambda^2 \sigma}{(4\pi)^3 R^4} \right] = \frac{\sigma}{R^4} \tag{2.2}$$

where P_r is the received power, P_t is the transmitted power, G_t is the gain of the transmitting antenna, λ is the radar wavelength, σ is the radar cross sections of the target and R is the distance from transmitter to target. In this case, we have to add the cross section of all the targets:

$$\sigma = \bar{\sigma} = V \sum \sigma_i = V\eta \tag{2.3}$$

$$\begin{cases} V & = scanned\ volume \\ & = pulse\ length \times beam\ width \\ & = \left[\frac{c\tau}{2}\right]\left[\frac{\pi R^2\theta^2}{4}\right] \end{cases} \quad (2.4)$$

where c is the light speed, τ is temporal duration of a pulse and θ is the beam width in radians. In combining the two equations:

$$P_r = \left[P_t \frac{G^2\lambda^2}{(4\pi)^3 R^4}\right]\left[\frac{c\tau}{2}\right]\left[\frac{\pi R^2\theta^2}{4}\right]\eta \quad (2.5)$$

$$P_r = \left[P_t \tau G^2 \lambda^2 \theta^2\right]\left[\frac{c}{512(\pi^2)}\right]\frac{\eta}{R^2} \quad (2.6)$$

This leads to:

$$P_r \propto \frac{\eta}{R^2} \quad (2.7)$$

Note: The return signal now varies inversely as R^2 instead of R^4. In order to compare the data coming from different distances from the radar, they have to be normalized with this ratio.

2.2 THE MICRO RAIN RADAR

Most meteorological radars are non-coherent type and are therefore used to observe the location and pattern of echoes and to measure the intensity of the backscattered signals. The Micro Rain Radar (MRR) is used to measure the vertical profiles of rain rate, liquid water content and drop size distribution. The Micro Rain Radar is an FM-CW (Frequency Modulated Continuous Wave) Doppler radar with a parabolic offset dish with 0.5 m efficient aperture diameter and 24.1 GHz transmit frequency. The CW-operation makes optimum use

of the available transmit power. Thus a stable and reliable Gunn oscillator with only 50 mW output power can be used for the transmitter. The retrieval of range-resolved Doppler spectra follows the method described by Strauch (1976).

Strauch (1976) demonstrated that Doppler radars based on the frequency modulated continuous wave (FM–CW) technique are able to measure height-resolved rain drop size distributions. The Micro Rain Radar is a highly reliable system suitable for use in remote and extreme environments, requiring minimal maintenance and is suited for long-term unattended operation. The Micro Rain Radar provides information for now-casting of precipitation; it will detect the start of rain from ground level to high above the radar level several minutes before the start of rain at ground level.

Unlike conventional weather Radars, the MRR does not provide areal coverage as it is operated only as a vertically looking profiler. The advantage of this operation mode is that the measured Doppler spectra can be transformed into number concentration versus drop size using the known relation between drop size and terminal fall velocity as suggested by Atlas *et al.* (1973).

The Micro Rain Radar output includes the rain rate, RR (mm/h), vertical structure of the radar reflectivity, z (dBZ), liquid water content, (g/m3), and falling velocity, v (m/s).

2.2.1 Radar-Frontend

The core component of the radar is a frequency modulated Gunn-diode-oscillator with integrated mixing diode. The nominal transmit power is 50 mW. The assembly and function of the radar frontend is explained with reference to the block diagram in Figure 1. The linear polarized radio - frequency -power is fed through a wave - guide and a horn, which represents the feed of an offset parabolic dish of 60 cm diameter. The backscattered signal is received

with the same antenna assembly. The received signal is then detected by a mixing diode, which is mounted in the wave guide between the Gunn-oscillator and horn. This diode, which is biased with a fraction of the transmit signal, acts as mixer. This simple configuration cannot be operated in pulsed mode because during the shut off of the transmitter; the receiver does not work either. When operated in continuous wave mode, a voltage appears at the diode output, which depends on the phase difference between the transmitting and receiving signal, and which is used for further signal processing (Metek, 2005).

2.2.2 Radar Frequency

The backscatter cross - section of rain drops increases with the fourth power of the radar frequency if the target diameter is small compared to the wavelength (Rayleigh scattering). This is why a high frequency is useful in order to increase the radar sensitivity with respect to small rain drops. At very high frequencies the quantitatively interpretable height range becomes limited due to attenuation at moderate and higher rain rates. At 24 GHz, which is used, attenuation effects may be noticeable but should be weak enough to be correctable with sufficient accuracy.

2.2.3 Radar Constant

The radar constant refers to the combination of radar system parameters and the physical constants that determine the proportionality factor between the reflectivity of a radar target at a given range and the power measured at the receiving antenna (America meteorological society glossary, 2007). The derived volume reflectivity, drop size distribution and all integral parameters depend on the proportionality of the radar calibration constant.

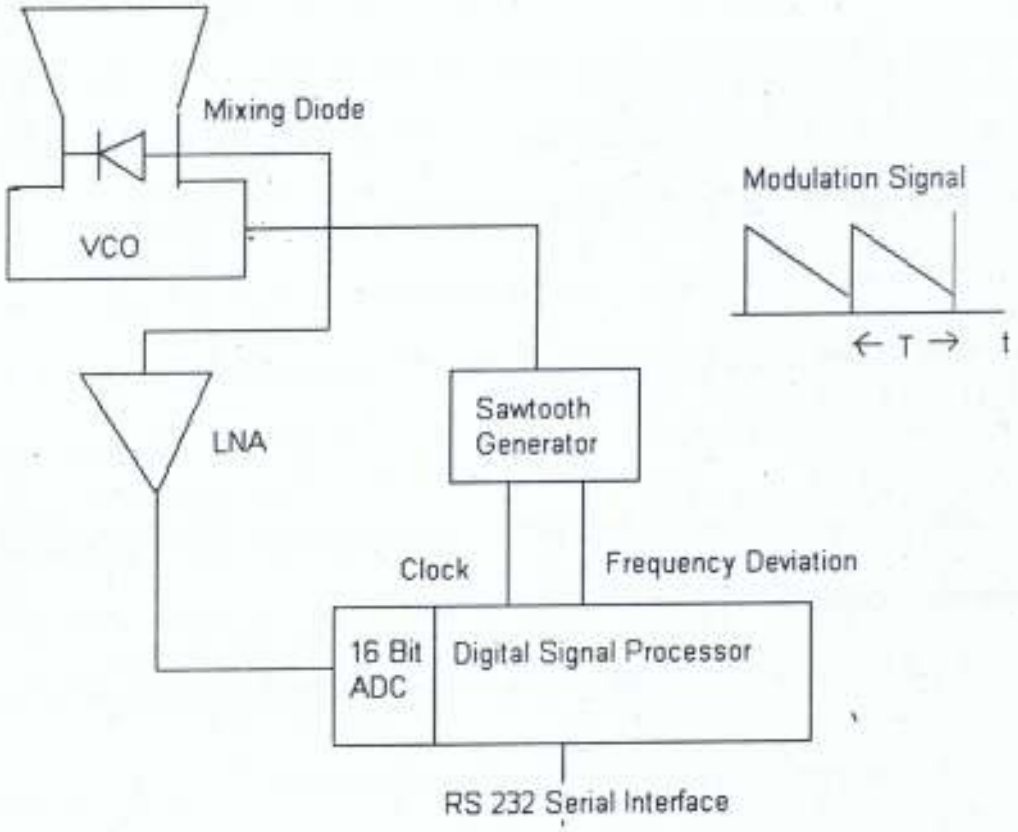

Figure 1: Block diagram of MRR

Due to the limited data rate of the serial interface of the MRR the minimum measuring cycle time has been set to 10 s. Issuing the spectra via the interface takes about 4 s, during this time no measurement is possible due to spurious interferences from the active data port to the low noise receiving amplifier. Thus 6 s measurement time is available with this setting of cycle time. 23 spectra per second are calculated and averaged incoherently which represent a mean of a minimum of 138 single spectra. The statistical fluctuations are reduced to about 9% of their mean values (METEK, 2005).

The Micro Rain Radar has the ability to measure drop spectra and rain intensity quantitatively by using the radar-retrieved data without any corrections produced rain intensities up to a factor of 3, which is considered too high, Löffler-Mang, et al., (1999).

Due to this inconsistency, Löffler-Mang et al., (1999) did several corrections. The electronic noise correction of the spectrum below 0.7-mm drop diameters decreased the rain intensity up to 20%. it was also shown that proper treatment of scattering by Mie theory decreased the rain intensity between 5% and 30%, depending on the spectrum width. The Micro Rain Radar was recalibrated by applying these improvements, and comparing the rain intensities of the Micro Rain Radar and a Joss – Waldvogel disdrometer for two days of stratiform rain, these led to new radar constant and to a decrease of rain intensity of 49%. A correlation coefficient of 0.94 was obtained. for the comparison of Micro Rain Radar and disdrometer rainfall data for a case study of one day.

2.2.4 Radar Resolution

Radar resolution is the radar's ability to display targets correctly. Both the azimuthal resolution and range resolution are problems that commonly affect all radars. Range resolution is the radar's ability to display in-line targets separately. Range resolution affects

targets along the beam, oriented behind one another. Targets must be more than one-half pulse length apart or they occupy the pulse together; their returned energy is merged making it impossible for the radar to see their separation. Targets closer together appear as one and are displayed accordingly (stretched along the beam axis). Range resolution is solely a function of pulse length and the pulse length is unaffected by distance, therefore the separation criteria remains constant.

Peters et al., (2002), found that the Micro Rain Radar could measure a rain rate of 0.1 mm h^{-1} comfortably and with reasonable accuracy within 1 min time-resolution, while the rain gauge would need 1hour to collect sufficient water for just one impulse. In reality, the rain gauge output would still be meaningless in such a situation.

Azimuthal resolution is often called bearing or directional resolution. It is radar's ability to display side-by-side targets correctly. Azimuthal resolution is controlled by beamwidth as only targets separated by more than one beam-width can be displayed separately. As the radar antenna rotates, targets too close together occupy the beam simultaneously. This causes them to be displayed as one wide target, stretched azimuthally (sideways). Since Azimuthal resolution depends on beam-width, which changes with distance, targets near the antenna require less separation than those further away. Near the antenna, a narrower beam allows the radar to recognize tighter gaps and display targets separately.

Diederich et al., (2004) found that the correlation with other instruments in drop numbers for drops smaller than 1mm remained low for Micro Rain Radar and the disdrometer in all situations, the reason being an extremely high noise level for Micro Rain Radar and probably horizontal wind for the Disdrometer. For drops larger than 1 mm, all instruments showed good correlation when rain variability and wind advection created similar conditions within the averaging time. The fact that the correlation was lowered noticeably when introducing

temporal offsets of ±1 min suggests that instrument precision is good enough to resolve temporal variability of rain contained in one minute. Longer averaging intervals smooth out variability, making it immeasurable for instruments with low sensitivity and long aggregation time such as rain gauges.

2.3 SHAPE OF FALLING RAINDROPS.

The size of raindrops ranges from very small to fairly large ones. The smallest drops may be equivalent to those found in clouds while the largest drops will not exceed 4 mm in radius since the drops with radii greater than 4mm are hydro-dynamically unstable and breakup (Oguchi, 1983).

The exact shape of a raindrop at any instant of time is influenced by a complex mixture of surface tension and aerodynamic forces as they fall to the ground. Four types of rain shapes have been recognized; spherical, elliptical, spheroidal and Pruppacher-Pitter (Ajewole, 1997). The raindrop size observed in this study ranges from 0.25 - 5.82 mm.

2.4 Drop Size Distribution

This refers to the rate of occurrence of raindrops sizes of a particular range in a rain event. It is an estimation of the proportion of raindrops per unit volume reaching the ground, contributed by raindrops of diameter interval "D" (Ajewole, 1997).

The raindrop size distribution can also be defined as the mean number of raindrops in a particular diameter interval present per unit volume of air $N_t(D)$ (mm^{-1} m^{-3}). However, there exists a second form of the raindrop size distribution, written as $N_A(D)$ (the subscript A standing for area), which can be defined as the mean number of raindrops in a particular diameter interval arriving at a surface per unit area and per unit time (Uijlenhoet and Stricker, 1999).

The corresponding units of $N_A(D)$ are $mm^{-1}\ m^{-2}\ s^{-1}$. The distinction between $N_I(D)$ and $N_A(D)$ is fundamental to a proper understanding of the concept of raindrop size distributions. Using the terminology of Smith (1993), $N_I(D)$ is the raindrop size distribution pertaining to the sample volume process and $N_A(D)$ that pertaining to the raindrop arrival process.

The knowledge of the drop size distribution (DSD) is of critical importance for the accurate retrieval of all rainfall parameters from weather radar data (Laura et al., 2006). Different models of raindrops size distribution were previously developed based on conditions in the temperate regions, but distributions most suited to tropical rainfall patterns were later developed. The earliest models developed include;

2.4.1 Laws and Parsons Distribution

In this method, Laws and Parsons (1943) made use of flour method, by exposing a pan containing fine flour to rain and the pellet formed by the raindrops was measured. A known relationship between the size of the dried pellet and the size of raindrops are used. They made extensive measurement in Washington DC for various rain types and found out that even for the same rain rate, the size distribution vary considerably from rain to rain, and hence they averaged the distribution for each rain rate.

The resulting drop size distribution obtained from the various volume distributions with a fall velocity $V(D)$ is

$$N(D) = \frac{10^3 R\beta(m)dD}{4.8\pi a^3 v(D)} m^{-3} \qquad (2.8)$$

Where R is the rain rate in mm/h, $\beta(m)dD$ is the volume percentage, 'D' is drop diameter, dD represents the size interval from $D - {}^{dD}/_{2}$ to $D + {}^{dD}/_{2}$

The Laws and Parson Distribution suitably represents actual condition in continental temperate region at the lower rain rate (50 mm/h).

Measurement of raindrops recorded on dyed filter papers were made for correlation with radar echoes (Marshall et al., 1947). These measurements were analyzed to give the distribution of drops with size; the distributions were in fair agreement with those of Laws and Parsons (1943).

Ajayi (1984), compared the raindrop size characteristics for one hour during the passage of a West Africa thunder squall system over Ile-Ife on 16th April 1982 to the monsoon rainfall on 7th September 1981 and found that raindrop size distributions at the beginning of the storm are remarkably different from those at the middle of the storm for equal rain rates. In addition, the drop size at the onset of the storm was characterized with greater number of large diameter drops, when compared with the distribution existing later in the storm. The observed differences can not be explained only in terms of the unequal terminal velocity of the small and large drops, but also as a result of the differences in the updraft velocities in the different parts of the storm. Such variation in the drop size distributions were absent during the monsoon rainfall.

Diederich et al., (2004) studied the variability in the drop size distribution inside an area of 200 by 600 m^2. Analyzing with a temporal resolution of 30 secs using 3 Micro Rain Radars, and 2 D-Video disdrometer, they found that the total Drop Size Distribution (DSD) accumulations as well as single radar reflectivity and rain rate values were calculated from DSDs obtained with one minute integration time in 22 drop size classes with 0.2 mm interval. The MRR DSDs were interpolated onto the same resolution for comparison, the calibration differences in the MRRs became apparent, as well as a large disagreement in the smallest drop classes. This disagreement between the MRRs was found to be caused by their different

noise levels and calibration. Noise subtraction affects mostly drop numbers in "slow" Doppler bins. The video Disdrometer counts significantly fewer drops at diameters between 0.2 mm and 0.6 mm, and more between 0.6 mm and 0.8 mm. A similar behavior was found for shorter integration times of a few hours, except that the disdrometer did not give realistic drop numbers lower than 10 $m^{-3}mm^{-1}$, whereas the MRRs continued to show agreeable drop numbers below 0.01 $m^{-3}mm^{-1}$. The disagreement for small drops was substantial enough to influence integral rain rate, Z/R ratio, total drop number and mean drop diameter, as well as the first Doppler moment (mean falling velocity) during the absence of larger drops.

2.4.2 Marshall and Palmer (Negative Exponential) Distribution

Marshall and Palmer (1948) proposed a simple negative exponential parameterization for the raindrop size distribution $N_v(D)$ as a fit to filter paper measurements of raindrop size spectra for rain rates between 1 and 23 mm/h,

$$N_v(D) = N_0 e^{-\Lambda D} \tag{2.9}$$

where, $\Lambda\,(mm^{-1})$ is the slope of the $N_v(D)$ curve on a semi logarithmic plot. An alternative interpretation of Λ is the inverse of the mean diameter of raindrops present in a volume of air (Uijlenhoet and Stricker, 1999). Marshall and Palmer found that N_0 was approximately constant for any rain rate, that is,

$$N_0 = 8.0\times10^{3} \tag{2.10}$$

and that Λ decreased with increasing rain rate $R(mm/h)$ according to the power law,

$$\Lambda = 4.1R^{-0.21} \tag{2.11}$$

Although the filter paper raindrop size measurements to which it was adjusted corresponded to rain rates not exceeding 23 mm/h, the Marshall-Palmer parameterisation has been found to remain a realistic representation of averaged raindrop size distributions for much higher rain rates (e.g. Hall and Calder, 1993) in temperate regions of the world.

Marshall and Palmer's exponential parameterization for the raindrop size distribution bears a functional dependence on only one variable, namely the rain rate R. In accordance with the terminology introduced by Sempere et al., (1994, 1998), this variable will be called the reference variable. The fact that the effective number of degrees of freedom of the raindrop size distribution equals one is fundamental to rainfall estimation using conventional (i.e. single-parameter) weather radar. If this were not the case, then Z would never contain enough information about the raindrop size distribution to yield a one-to-one power law relationship with (that is, a direct functional dependence on) R.

Sempere et al., (1994), proposed a general formulation for drop size distribution in terms of a scaling law that is able to reproduce and interpret all previous studies dealing with drop size distribution. This provides a general frame work where the classical role of the rain intensity as the reference variable can played by any integral rainfall variable without the generality of the expression being modified.

This distribution is especially in agreement with the Laws and Parson (1943) distribution that was obtained experimentally. It however tends to overestimate the density of raindrop size below 1.5 mm diameter due to the exponential increase in the density as the raindrop radius 'a' tends to zero.

2.4.3 Modified Gamma Distribution

Deirmendjian (1969) proposed a modified form of the negative exponential distribution expressed in the form

$$n(D) = N_0 D^{-m} e^{-\Lambda D^{\beta}} \qquad (2.12)$$

where N_0, m, Λ, β are positive real constants.

This distribution corrects the tendency of n (D) to blow up as "D" tends to zero. Obtaining the constants N_0, Λ, m, and β from practical experiment is however difficult.

When the value of m is the range 3-5, the modified gamma distribution tends to underestimate both large and small ends of the drop size spectrum (ITU-R., 1995).

2.4.4 Joss et al Distribution

Joss et al., (1968) took measurement at Loreano, Switzerland using disdrometer. They observed a significant variation in the distribution across the different rain types. The parameters of the average exponential distribution have been obtained for different types of rain. These are as shown in Table 2.1

Table 2.1: The parameters of Negative Exponential Rain drop size Distributions of Joss et al., (1968)

Types of rain	N_0 ($m^{-3}mm^{-1}$)	Λ (mm^{-1})
Drizzle	6×10^{-4}	$11.4R^{-0.21}$
Widespread	1.4×10^{-4}	$8.2R^{-0.21}$
Thunderstorm	2.8×10^{-3}	$6R^{-0.21}$

2.4.5 Lognormal Distribution.

A number of investigators of raindrop size proposed the lognormal distribution model. Ajayi and Olsen (1985), using the lognormal function theoretically fit data collected at Ile-Ife, Nigeria by the use of moment regression technique to obtain,

$$N(D) = \frac{N_T}{\sigma D\sqrt{2\pi}} e^{-\left(\frac{\ln(D)-\mu}{2\sigma}\right)^2} \qquad (2.13)$$

where μ is the mean of In(D), σ is the standard deviation of In(D), D is the rain drop diameter and N_T is the total number of drops of all sizes. The parameters μ, σ and N_T are dependent on climate, geographical location and rain type.

Maitra and Gibbins, (1999) used the lognormal and gamma distribution techniques for modeling the distribution of raindrops size for the measurement of rain attenuation at two frequencies and rain rate. The lognormal distribution is compared with the two-parameter gamma distribution with a fixed value of index obtained from measurements of rain attenuation at infrared wavelength and rain rate. From the analysis of the two rain events, it was found that the agreement between measured attenuation and calculated attenuation using lognormal distribution is good and some better than that using the gamma distribution. The gamma distribution yields higher number densities for small drops than those given by the lognormal distribution, which may not be realistic.

2.4.6 Spatial and Temporal Variability of the Drop Size Distribution.

Curtis et al., (1999) considered two case examples; one for North Palm Beach, Florida, USA for January 2, 1999, and the other one for San Diego. Rainfall topologies were derived using inverse distance squared weighting, the Kriging and Radar methods. The inverse distance

squared weighting technique provided contours that are strongly circular in nature, particularly in the immediate vicinity of the local maxima and minima. While the other procedures used for grid-based rainfall estimation is that of Kriging (Kitandis, 1997), which produces contours that are somewhat less artificial looking than the inverse distance squared method. While the Radar analysis showed rainfall contours elongated along a line from the Southwest to North East with a significant side lobe to the South East of the storm centre. Animation of the entire storm event shows that during the early stages of the event, rain cells migrated from the South East to the general location of the storm centre, stalled, then exploded in intensity before drifting off to the North East. None of this is indicated from the analysis of rain gage data from the same locations.

2.5 RAINFALL TYPES

There are two main types of rainfall; these are stratiform and convective. Stratiform rainfall consists of the drizzle and widespread rain while convective rainfall consists of the shower and thunderstorm rain (Joss et al., 1968). The difference between these types usually lies in the maximum rain rate to be associated with the rain process but not with the difference in spatial and variability (ITU-R, 1995).

The drizzle is a low intensity rainfall of about 5 mm/h, it is associated with drops of diameter of the order of 1.0 mm. They may be generated by the stratus cloud (Adediji, 2003).

Widespread rainfall has intensity of about 50 mm/h and the duration is usually long and greater than an hour. Widespread rain consists of raindrops with diameters in the range of 1.0-3.5 mm; it occurs fairly steadily and uniform over relatively large areas.

Shower rainfall is often called warm rain and consists of extremely few raindrops above 2.0 mm diameter. It occurs suddenly with small duration of between 10-15 minutes. It originates

very well from below the 0°C isotherm height and so they do not involve the ice phase. It is characterized by high rainfall intensity of about 150 mm/hr and is generated within the Cumulus cloud.

The thunderstorm rain is generated within the cumulonimbus cloud (high rising clouds). Thunderstorm rain is characterized by high rainfall intensity sometimes in excess of 120 mm/hr with relative high concentration of large drops typically greater than 3.00 mm. Thunderstorm rain is sometimes accompanied by thunderstorm activities especially in the tropics.

2.6 RAINFALL RATE

This is a measure of the intensity of rainfall by calculating the amount of rain that would fall over a given interval of time if the rainfall intensity were constant over that period of time. The rate is typically expressed in terms of length (depth) per unit time, for example, millimeters per hour, or inches per hour (AMS, 2007).

Battan (1973) gave the contribution of water or ice particle of mass M_i to the precipitation rate, R_i as;

$$R_i = M_i(w_i - w_a) \tag{2.14}$$

where w_i is the terminal velocity of the drop and w_a is the updraft rate. Computing the precipitation rate from a unit volume of air, the value of R_i is integrated over all drops in the volume. When all particles have the same size, the precipitation rate can be written as

$$R = \frac{4}{3}\pi\rho a^3 N(w - w_a) \tag{2.15}$$

Where N is the concentration of particles of density ρ. In general

$$R = \frac{4}{3}\pi\rho \int_{a=0}^{a=\infty} a^3 N(a)(w_a - w_u)da \qquad (2.16)$$

where w_a is a fraction of raindrop radius a, $N(a)\,da$ is the number of particles of radius between a and $a + da$ per unit volume.

The rain rate calculated from the Micro Rain Radar Doppler spectrum agrees better with in-situ precipitation measurements than any constant Z-R power law, Diederich, (2004). This was tested by deriving precipitation sums with one hour integration time, and calculating the correlation coefficient between rain gauges and Micro Rain Radar for Drop Size Distribution and Z-R rain rates. The correlation with gauges was 0.98 for rain rates derived from the Drop Size Distribution, and 0.94 for the best Z-R relation.

Diederich et al., (2004), showed that for total rainfall accumulations over periods longer than several days, three rain gauges showed smaller deviations from each other (below 5%) than three Micro Rain Radars (more than 10%). This was not only caused by calibration errors but also by the dissimilar behaviours of different Micro Rain Radars in the noise correction at the "slower" end of the Doppler spectrum.

Löffler-Mang et al., (1999), showed that the Micro Rain Radar reliability was good for the first year of operation, only a few minutes of data were lost when saturation occurred at high rainfall intensities above 50 mmh^{-1}. Furthermore, the daily rain sums between November 1996 and April 1997 derived from the Micro Rain Radar at a measurement height of 100 m above ground were on average 12% higher than measurements with a conventional Hellmann-type rain gauge. A comparison of the daily sums of precipitation for this 1-yr period confirms and strengthens the result of the case studies: the Mie correction substantially reduces the errors of the radar measurements, resulting in an excellent performance in measuring daily rainfall with the Micro Rain Radar.

2.7 RADAR REFLECTIVITY

This is a measure of the efficiency of the radar target in intercepting and returning radio energy. It depends upon the size, shape, aspect, and dielectric properties of the target.

It includes not only the effects of reflection but also scattering and diffraction. In particular, the radar reflectivity of a meteorological target depends upon such factors as; the number of hydrometeors per unit volume, the size distribution of the hydrometeors, the physical state of the hydrometeors (ice or water), the shape or shapes of the individual elements of the group, and if asymmetrical, their aspect ratio with respect to the radar (America meteorological society glossary, 2007).

The weather radar equation describes the relationship between the received power, the properties of the radar, the properties of the targets and the distances between the radar and the target. In this treatment, the targets are assumed to be raindrops. At non-attenuated wavelengths (Battan, 1973), the weather radar equation becomes

$$\overline{P_r} = C \frac{|K|^2}{r^2} Z \qquad (2.17)$$

where $\overline{P_r}$ is the mean power received from raindrops at range r (km), C is the so-called radar constant, $|K|^2$ is a coefficient related to the dielectric constant of water (~ 0.93) and Z (mm^6 m^{-3}) is the radar reflectivity factor, hereafter simply referred to as radar reflectivity. All radar properties are contained in C, and all raindrop properties in $|K|^2$ and Z. Z is related to the size distribution of the raindrops in the radar sample volume according to Battan, (1973) as

$$Z = \int_0^\infty D^6 N_r(D) dD \qquad (2.18)$$

where $N_v(D)dD$ (the subscript v stands for volume) represents the mean number of raindrops with equivalent spherical diameters between D and $D + dD$ (mm) present per unit volume of air. The corresponding units of $N_v(D)$ are $mm^{-1}\ m^{-3}$. Hence, although Z is called the radar reflectivity factor, it is a purely meteorological quantity that is independent of any radar property. The radar reflectivity η has dimensions of area per unit volume (e.g., cm^2m^{-3}, or, more commonly, cm^{-1} or m^{-1}) and is defined by

$$\eta = \sum N_i \sigma_i \tag{2.19}$$

where N_i is the number of hydrometeors per unit volume with backscattering cross section σ_i and the summation is over all the hydrometeors in a unit volume. For spherical hydrometeors small enough compared with the wavelength or under the so-called Rayleigh scattering approximation, the radar cross section is related to particle size by

$$\sigma = \frac{\pi^5 |K|^2 D^6}{\lambda^4} \tag{2.20}$$

where λ is the wavelength, D the diameter of the hydrometeor, and K the dielectric factor defined as

$$K = \frac{m^2 - 1}{m^2 + 2} \tag{2.21}$$

where m is the complex index of refraction of the hydrometeor.

Diederich et al., (2004), compared the vertical reflectivity profiles measured by the Micro Rain Radars to that of weather radar volume scans at different beam heights, as well as that of vertically pointing 35 GHz cloud radar and Transportable Atmospheric Radar. All Micro Rain Radars displayed a loss in intensity of about −2 dBZ per kilometre altitude, relative to the 35 GHz cloud Radar and weather radar volume scans, which is in agreement with the

The radar effective reflectivity, (Z_e) varies as the 6th power of the rain droplet diameter (D), the square of the dielectric constant (K) of the target and the drop size distribution (e.g. $N[D]$ of Marshall-Palmer) of the drops. This gives a truncated Gamma function, of the form:

$$Z_e = \int_0^{D\max} |K|^2 N_0 e^{-\Lambda D} D^6 dD \qquad (2.22)$$

Since variation in diameter and dielectric constant of the targets can lead to large variability in power return to the radar, reflectivity is expressed in *dBZ* (10 times the logarithm of the ratio of the echo to a standard 1 mm diameter drop filling the same scanned volume) (Battan, 1973).

. Therefore reflectivity in *dBZ* is given by the expression:

$$Z = 10Log_{10}\left(\frac{z(mm^6/m^3}{1(mm^6/m^3}\right) \qquad (2.23)$$

2.7.2 Vertical Variation of Reflectivity

Profiles of the radar reflectivity factor Z as a function of height for a given value of Z at the surface display little change below a certain transition height (ITU-R, 1995).

The region below the transition height is predominantly rain and contributes to both attenuation and scattering. For stratiform rain a distinct narrow layer of enhanced reflectivity exists at around the transition height; the dimension of this layer is on average about 300 m but can some time reach values of up to 1 km (Hines et al., 1983). This layer is known as the melting layer or the bright band. Profile of the reflectivity Z above the transition height; show a decrease with height that appears to depend on climate. The slope just above the transition height varies between about 3 - 9 dB/km. The slope is expected to become steeper at higher

results of a previous comparison between Micro Rain Radar and weather radar of the Deutsche Wetterdienst (DWD). During separate test runs, 2 Micro Rain Radars were operated with different range resolutions, which led to a bias of about 1 dBZ/km, if the range resolution of one was doubled. The profiles showed a bias of less than 0.3 dBZ/km when operating at identical range resolution.

Ulbrich et al., (1998), compared the extent to which variations in Z–R (reflectivity factor–rainfall rate) relations can explain the systematically large offsets of radar-measured rainfall from rain gauge measurements as observed with some National Weather Service Project WSR-88D radars. They compared the reflectivity factors found from disdrometer data with those measured by the National Weather Service (WSR-88D) radar at Greer. The work demonstrated that the latter radar measured reflectivity factors that are at least 3.5 dB too small when compared with the disdrometer data. This systematic offset in radar-measured reflectivity factors is shown to be consistent with the factor of 2 underestimation of rainfall amounts commonly observed with the Greer radar when compared with a well maintained network of rain gauges. Since similar deviations of radar-measured rainfall amounts from rain gauge data have been observed with National Weather Service (WSR-88D) radars at several other locations, this work suggests that these differences are probably due to calibration offsets.

2.7.1 Reflectivity in decibel or dBZ

The Return echoes from targets, are analyzed for their intensities in order to establish the precipitation rate in the scanned volume. The wavelengths used (1 to 10 cm) ensure that this return is proportional to the rate because they are within the validity of Rayleigh scattering which assumes that the targets must be much smaller than the wavelength of the scanning wave (by a factor of 10).

The radar effective reflectivity, (Z_e) varies as the 6th power of the rain droplet diameter (D), the square of the dielectric constant (K) of the target and the drop size distribution (e.g. $N[D]$ of Marshall-Palmer) of the drops. This gives a truncated Gamma function, of the form:

$$Z_e = \int_0^{D\max} |K|^2 N_0 e^{-\Lambda D} D^6 dD \qquad (2.22)$$

Since variation in diameter and dielectric constant of the targets can lead to large variability in power return to the radar, reflectivity is expressed in *dBZ* (10 times the logarithm of the ratio of the echo to a standard 1 mm diameter drop filling the same scanned volume) (Battan, 1973).

. Therefore reflectivity in *dBZ* is given by the expression:

$$Z = 10Log_{10}\left(\frac{z(mm^6/m^3)}{1(mm^6/m^3)}\right) \qquad (2.23)$$

2.7.2 Vertical Variation of Reflectivity

Profiles of the radar reflectivity factor Z as a function of height for a given value of Z at the surface display little change below a certain transition height (ITU-R, 1995).

The region below the transition height is predominantly rain and contributes to both attenuation and scattering. For stratiform rain a distinct narrow layer of enhanced reflectivity exists at around the transition height; the dimension of this layer is on average about 300 m but can some time reach values of up to 1 km (Hines et al., 1983). This layer is known as the melting layer or the bright band. Profile of the reflectivity Z above the transition height; show a decrease with height that appears to depend on climate. The slope just above the transition height varies between about 3 - 9 dB/km. The slope is expected to become steeper at higher

altitudes. The transition height is expected to be closely related to the height of the 0°C isotherm, which depends on the latitude, climate and season.

For stratiform precipitation seasonal variation of this height has been seen to be correlated with ground temperature (Fujita et al., 1979).

2.7.3 Reflectivity on a Radar Display

Radar returns are usually described by colour or level. The colours in a radar image normally range from blue or green for weak returns, to red or magenta for very strong returns. The numbers in a verbal report increase with the severity of the returns (America meteorological society glossary 2007).

For example, the U.S. National Doppler Radar sites use the following scale for different levels of reflectivity:

(A) Magenta: 65 dBZ (extremely heavy precipitation)

(B) Red: 52 dBZ

(C) Yellow: 36 dBZ

(D) Green: 20 dBZ (light precipitation)

Strong returns (red or magenta) may indicate not only heavy rain but also thunderstorms, hail, strong winds, or tornadoes, but they need to be interpreted carefully.

2.8 Z-R RELATIONSHIP

Remote measurement of the rainfall rate R is of considerable practical interest. For many years meteorologists have attempted to find a useful relationship between the radar

reflectivity factor Z and the rainfall rate R. Unfortunately, there is no single relation that can satisfy all meteorological phenomena.

Battan (1973) lists no fewer than 69 separate Z-R relationships that have been proposed by various investigators. More importantly, observed drop size distributions of which both Z and R are functions could be expressed in an indefinite number of parameters. Single parameter measurement of rainfall constrains the DSD to one free parameter, which may vary strongly in both space and time. Droplets of natural clouds and precipitation satisfy the condition of Rayleigh approximation, namely that the diameter is much smaller than the wavelength, for wavelengths used in weather radars (Sauvageot, 1992). If it is assumed that a radar can monitor certain atmospheric phenomena, then the radar reflectivity factor (Z) can be related to the relevant physical quantities. Many works were performed relating rainfall rates (R) and Z, resulting in a general function of the form:

$$Z = aR^b \tag{2.24}$$

where Z is given in mm ^{6} m $^{-3}$, R in mm h^{-1} and a and b are coefficients which depend on the raindrop number distribution $N(D)$ as function of the drops diameter (D) and type of precipitations (rain), (convective or stratiform). Several methods have been proposed to establishing the Z-R relationship. One of them requires a disdrometer for measuring a set of $N(D)$ (Joss and Waldvogel, 1967 and 1969; Campistron, et al., 1987). In others, Z and R are measured simultaneously and independently by radar (Z) and rain gage network (R). Theoretical values of a and b coefficient can be either computed using the $N(D)$ distributions or taken from literature with certain restrictions.

As the antenna scans the atmosphere, on every angle of azimuth it obtains a certain number of returns from each target encountered. Reflectivity is then averaged for that target in order to have a better data set.

2.9 ATTENUATION BY RAIN

Attenuation is an important consideration in the modern world of wireless telecommunication. People are daily affected by it, as they rely more and more on mobile phones, television, satellite communication, and wireless internet. Attenuation limits the range of radio signals and is affected by the materials a signal must travel through (e.g. air, wood, concrete, rain).

Attenuation by Rain is one of the major problems in utilization micro wave and millimeter wave band for terrestrial and space communication purposes. Rain drops can absorb and scatter electromagnetic energy and attenuation thus introduced can often exceed the acceptable level of the communication systems Oguchi (1983).

Ryde (1944) developed a general procedure of obtaining theoretical relationship between attenuation and rain rate. The equation governing the variation of wave intensity I along a direction Z for a plane wave propagating in a rain medium is given by the equation:

$$\frac{dI}{dz} = -(\sum Q_i)I \tag{2.25}$$

where $\sum Q_i$ is the sum of the total cross section of all the raindrops in a unit volume in space. This implies that the rate of decrease of wave intensity in a thin slab of thickness dz is proportional to the energy absorbed in and scattered from the raindrops in the slab.

Therefore the intensity I is:

$$I = I_0 e^{-(\sum Q_i)z} \tag{2.26}$$

where I_0 is the intensity at $z = 0$

$$\sum Q_i = \int Q_i(a)n(a)da \tag{2.27}$$

where $n(a)da$ is the drop size distribution and is a function of rain rate R. Thus attenuation of the wave intensity A, when the wave passes though a rain slab of 1 km thickness is given by:

$$A = 4.343 \times 10^3 \times \int Q_t(a) n(a) da \quad \text{(dB/km)} \tag{2.28}$$

where A is given in positive decibel value.

Ajayi et al., (1984), analyzed rainfall attenuation using rainfall intensity measurement at Ile-Ife, southern Nigeria. The results obtained with three different expressions for rain height showed that a rain height of 3 km is a reasonable assumption for estimating earth-space rainfall attenuation at the location. They also found that for frequencies above 200 GHz, the polarization dependence of the specific attenuation due to rainfall becomes negligible.

The specific rain attenuation model for prediction methods has been recommended by the ITU-R. The specific attenuation γ_R (dB/km) for rain was recommended to be obtained from the power-law relationship:

$$\gamma_R = \mathrm{a} \, . \, \mathrm{R}^b \tag{2.29}$$

where "a" and "b" are power-law parameters, and R is the rain rate in mm/h.

Wei-Zhang et al., (2000), recommended the usage of an expanded set of power-law parameters in calculating the specific attenuation due to rain. This expansion is needed to accommodate an expanded set of raindrop size distributions, because the raindrop size distribution changes with geographical location and can strongly influence rain attenuation. Generally, the power-law parameters for Laws and Parsons (L - P) and Marshall and Palmer (M - P) distributions are used for estimating specific attenuation due to rain. It was suggested, however, that it is more reasonable to use a gamma raindrop size distribution for high latitude locations and a lognormal raindrop size distribution for tropical regions. It was further shown

that the specific attenuation for Laws and Parsons Raindrop size distribution is nearly the same as the specific attenuation obtained from power-law parameters of the ITU-R model, Wei-Zhang (2000).

CHAPTER THREE

PROJECT SITE, INSTRUMENTATION AND METHODOLOGY

3.1 PROJECT SITE

The measurement site chosen for the study is the Federal University of Technology Akure Ondo State Nigeria (7°15'N, 5°15'E) (fig.3.1). The measurement was taken for a period of two years 2006 and 2008.

3.2 INSTRUMENTATION

The instrument employed in taking the measurement is the Micro Rain Radar shown in Figure 3.2. The antenna is simultaneously used for the transmission of the RADAR signals and receiving of backscattered signals from the raindrops. It is designed as an offset parabolic dish. The angular aperture is approximately 2°. The parabolic dish is fastened together with the electronics unit and the RADAR module through the antenna mounting. The use of a parabolic dish allows a vertical alignment of the antenna beam without the need of a horizontal alignment. The antenna is positioned so as to allow rainwater drain off without retaining it.

The electronics unit shown in Figure 3.3 generates the RADAR transmitting signal and passes it to the RADAR module. It analyses the backscattered received signal and transfers the data to the connected control and evaluation computer, where the Doppler spectra are computed.

The electronics unit is located in a water protected IP65 housing, which is fixed to the antenna mounting. At the bottom side of the electronics unit there is a socket for the cable leading to the connection box/power supply.

The connection box shown in Figure 3.4 with the aid of a 25-pin D-sub-miniature socket female type (fig. 3.5) is used to pass the data through to the controlling computer. A flanged socket (fig. 3.6) is used for connecting RADAR electronics unit box (fig. 3.3) to the connection box, the power supply is also integrated in the connection box.

The vertical profile of the rain rate, liquid water content, fall velocity, radar reflectivity factor and drop size distribution up to 4800 m-height above sea level were then measured using the Micro Rain Radar at height levels 160 m steps above the radar.

The rain events were sampled with one minute time resolutions and stored subsequently as one minute averages for all the measured parameters.

3.3 PRINCIPLE OF MEASUREMENT OF THE MICRO RÀIN RADAR

The measuring principle of the Micro Rain Radar is based on electromagnetic waves of a frequency of 24 GHz. In contrast to normal rain-radar devices, the signals are emitted vertically into the atmosphere. A part of the emitted signal is scattered back to the parabolic antenna by the rain drops. The output signal is transmitted continuously (continuous wave, CW mode in contrast to pulsed radars). The Micro Rain Radar is a Doppler radar, that is, when falling to the ground the rain drops move relatively to the antenna on the ground, which act as both transmitter and receiver. Due to the falling velocity of the rain drops relative to the stationary antenna there is a frequency deviation between the transmitted and the received signal known as Doppler frequency. This frequency is a measure of the falling velocity of the rain drops. Since rain drops of different diameter have different falling velocities (Atlas et al., 1973), the backscattered signal consists of a distribution of different Doppler frequencies. The spectral analysis of this signal yields a wide distribution of lines corresponding to the Doppler frequencies of the signal.

The Radar electronics determines this spectrum with a high time resolution of 10 seconds and sends it to the connected control and data acquisition system, where the drop spectrum is calculated from the Doppler spectrum considering the transfer function of the radar module. The integration over the entire drop spectrum, considering further correction terms, followed by an averaging for 30 seconds, results in the actual rain rate and the liquid water content.

The Micro Rain Radar measures the Doppler spectrum from 0 to 12 m/s. The standard real-time processing uses the relation given by Atlas et al., (1973) to attribute drop diameters to Doppler velocities.

Mie theory is then used to calculate the rain drop numbers from the spectral volume reflectivity. Corrections for oblate rain drops and lower air densities leading to higher falling velocities in high altitudes are applied. The Rain Drops Size Distribution (DSD) is then calculated for falling velocities from 0.78 to 8.97 m/s in 43 intervals, corresponding to drop diameters from 0.245 to 4.530 mm, which is the range where the signal to noise ratio is considered adequate. Appropriate attenuation correction for moderately high rain rates is done by calculating Mie extinction from the derived DSD. Rain rate, Liquid water content LWC, and Rayleigh reflectivity Z are calculated from the DSD, while the mean falling velocity (first Doppler moment) and integral reflectivity (zeroth Doppler moment) are calculated directly from the measured Doppler spectrum. The Micro Rain Radar range resolution can be set from 10 to 200 m in 30 height intervals. Attenuation at 24 GHz prevents the use of ranges higher than 6 km. The averaging time for one measurement can be set from 10 s up to several hours (3600 s).

3.4 DATA SOURCE

In-situ measurements of the rainfall parameters were made in 2006 and 2008. The data were collected for 30 different range gates, from 0-160 metres above sea level (sea level height in Akure is 350 m) in a step of 160 m up to 4800 m. A typical measured data is shown in Table 3.1.

3.5 DERIVATION OF RAIN DROPS SIZE DISTRIBUTION.

The drop size distribution was derived from the raw power received by the radar given as

$$p(f_D)\Delta f_D = C(r)\frac{1}{r^2}\frac{1}{\Delta h}\eta(f_D)\Delta f_D \qquad (3.1)$$

where Δh is the range (height) resolution, r is the number of the range gate, $C(r)$ is a calibration function containing radar specific parameters, and $\eta(f_D)\Delta f_D$ is the spectral reflectivity density, that is, the backscatter cross section per volume and per frequency. Δf_D is the frequency resolution. The Doppler Spectra are resolved into 64 lines as

$$\eta_{nn} = 10^{F_{nn}/10} \qquad (3.2)$$

where "nn" indicates the line number ($0 \le nn \le 63$). F_{nn} is called "logarithmic spectral volume reflectivity. The "spectral reflectivity" density is then defined as:

$$\eta(f_{D,nn}) = \frac{\eta_{nn}}{\Delta f_D} \qquad (3.3)$$

where $\Delta f_D = 30.52Hz$

using the generalized form, in which a height dependent density correction for the fall velocity dv(h) Atlas (1973) is defined as:

$$v(D)m/s = (9.65 - 10.3\exp(-0.6D))\partial v(h) \quad \text{for } 0.109 \le D \le 6\text{mm} \qquad (3.4)$$

Using the America Standard Atmosphere conditions for the height dependence of air density and making use of the relation of Foote and duToit (1969), $\partial v(h)$ under these assumptions is defined as:

$$\partial v(h) = \left[1 + 3.68 \times 10^{-5} h + 1.71 \times 10^{-9} h^2\right] \tag{3.5}$$

The spectral reflectivity can be calculated from the drop diameter using the expression:

$$\eta(D_m) = \eta(f_{D,m}) \frac{\partial f_D}{\partial v} \frac{\partial v}{\partial D} \tag{3.6}$$

where

$$\frac{\partial f_D}{\partial v} = 160.1973 m^{-1} \tag{3.7}$$

and

$$\frac{\partial v}{\partial D}\left(ms^{-1} mm^{-1}\right) = 6.18 \times \exp(-0.6D)\partial v(h) \tag{3.8}$$

Substituting equation (3.7) and (3.8) into (3.6) gives:

$$\eta(D_m) m^{-1} mm^{-1} = \eta(f_{D,m}) \times 990.02 \times \exp(0.6 mm^{-1} D) \tag{3.9}$$

Dividing equation (3.9) by $\sigma(D_m)$ gives:

$$N(D_m) = \frac{\eta(D_m)}{\sigma(D_m)} \tag{3.10}$$

where $N(D_m)$, is the Drop size distribution and $\sigma(D_m)$ is the single particle backscattering cross section of rain drop of diameter D_m.

3.6 EQUIVALENT RADAR REFLECTIVITY FACTOR

The equivalent radar reflectivity factor is defined by

$$Z_e = \frac{\lambda^4}{\pi^5} \frac{1}{|K|^2} \int_0^\infty \eta(f_{D,m}) \partial f_D \tag{3.11}$$

In the limit of small drops (Rayleigh approximation), Ze is equal to the 6^{th} moment of the drop size distribution

$$Z = \int_0^{\infty} N(D) D^6 dD \qquad (3.12)$$

Z is calculated on the basis of the drop size distribution measured by the Micro Rain Radar using equation 3.12.

3.7 RAIN RATE

This is the rate at which water reaches the ground or the rate of accumulation of water per unit time (mm/h). The differential rain rate is equal to the volume of the differential droplet number density multiplied with the terminal falling velocity *v(D)*.

$$\left(\frac{\pi}{6} N(D) D^3\right) \qquad (3.13)$$

From this product the rain rate is obtained by integrating over the drop size using the formula:

$$RR = \frac{\pi}{6} \int_0^{\infty} N(D) D^3 V(D) dD \qquad (3.14)$$

3.8 LIQUID WATER CONTENT (LWC)

The liquid water content is the product of the total volume of all droplets with the density of water ρ_w, divided by the scattering volume. It is therefore proportional to the third moment of the drop size distribution. This is calculated by using the formula given below:

$$Lwc = \rho_w \frac{\pi}{6} \int_0^{\infty} N(D) D^3 dD \qquad (3.15)$$

3.9 CALCULATION OF RAIN ATTENUATION

Attenuation is calculated using the power law relation:

$$A = aR^b \qquad (3.16)$$

where "a" and "b" are the power law parameters which have been studied and calculated theoretically by many investigators. Ajewole et al., (1999), calculated these power law parameters for a tropical region, for the frequency range of 1–100 GHz. Using the rain rate measured by the MRR, the specific attenuation was calculated for the frequencies 1 – 100 GHz.

3.10 Z-R AND M-R RELATIONSHIPS

Equation 2.24 was used to determine the relationship between rainfall rate (R), radar reflectivity factor (Z) and Liquid water content (M) by making rainfall rate the independent variable. Natural logarithm is applied to both sides of the equation resulting in:

$$LnZ = Lna + bLnR \qquad (3.17)$$

Comparing equation (3.17) with a straight-line function;

$$Y = \alpha + \beta X \qquad (3.18)$$

where α and β are the y-axis intercept and the slope respectively. The coefficients a and b of equation 2.24 were estimated by linear regression for Z versus R and M versus R.

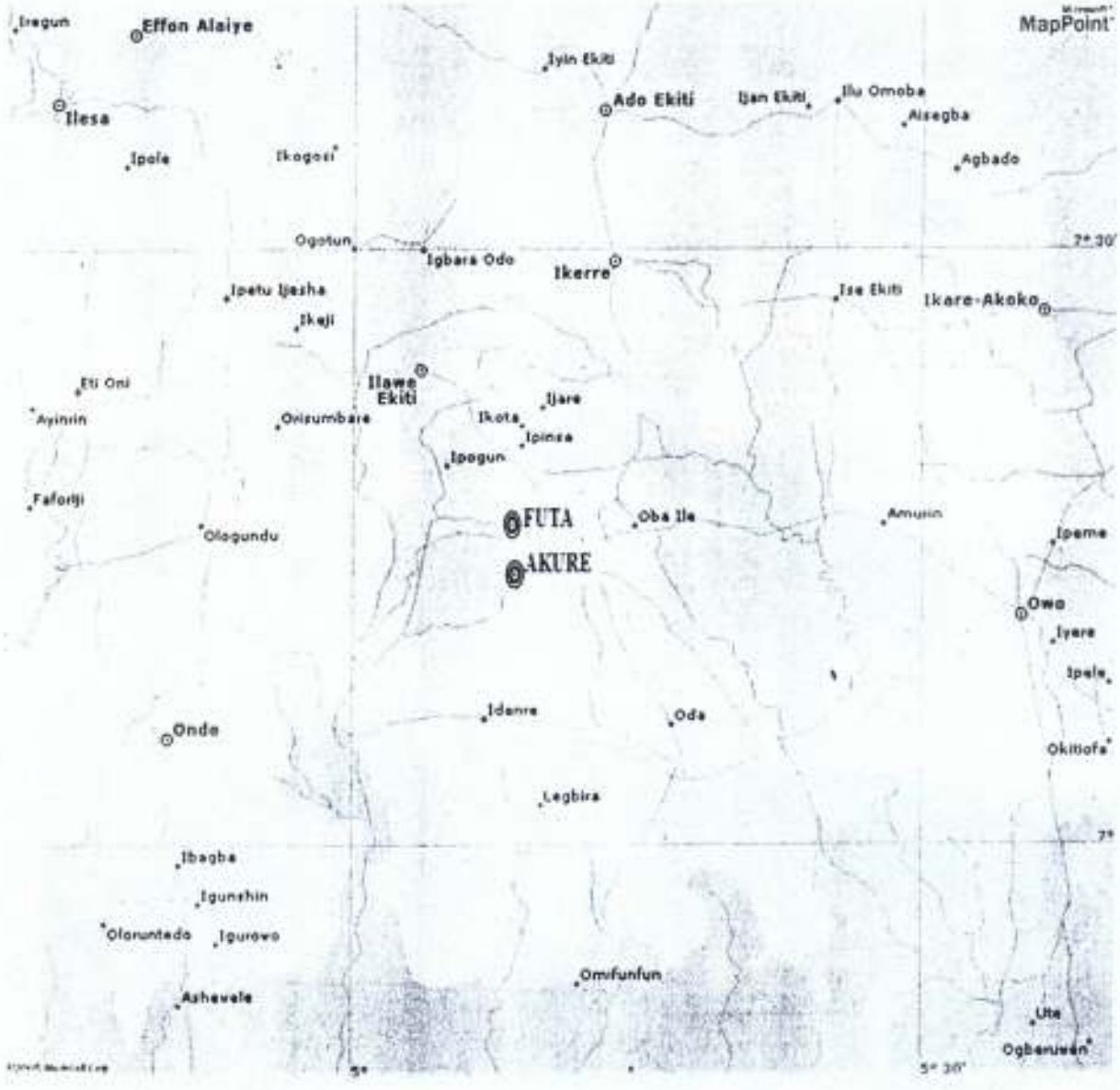

Fig. 3.1: Map of Ondo state, Nigeria showing where data was collected

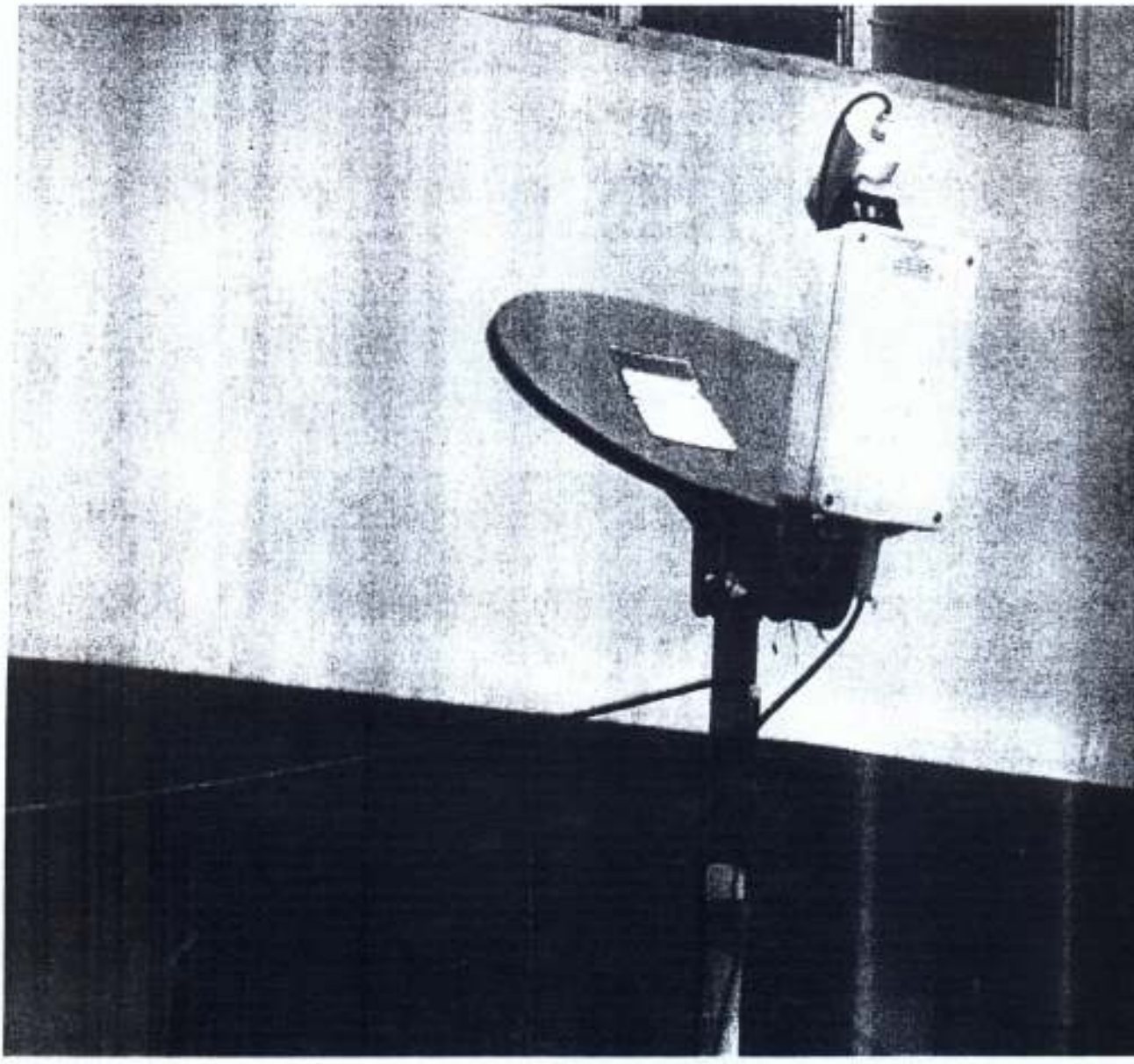

Fig. 3.2: Outdoor unit of the Micro Rain Radar installed in Physics Department, FUTA.

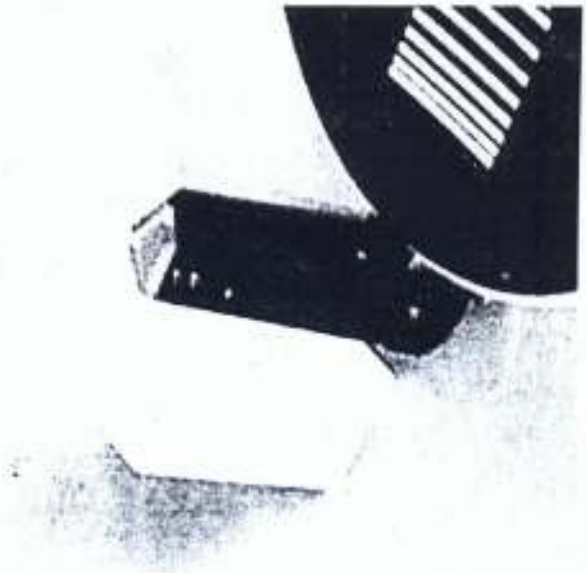

Fig. 3.3: RADAR Electronics Unit

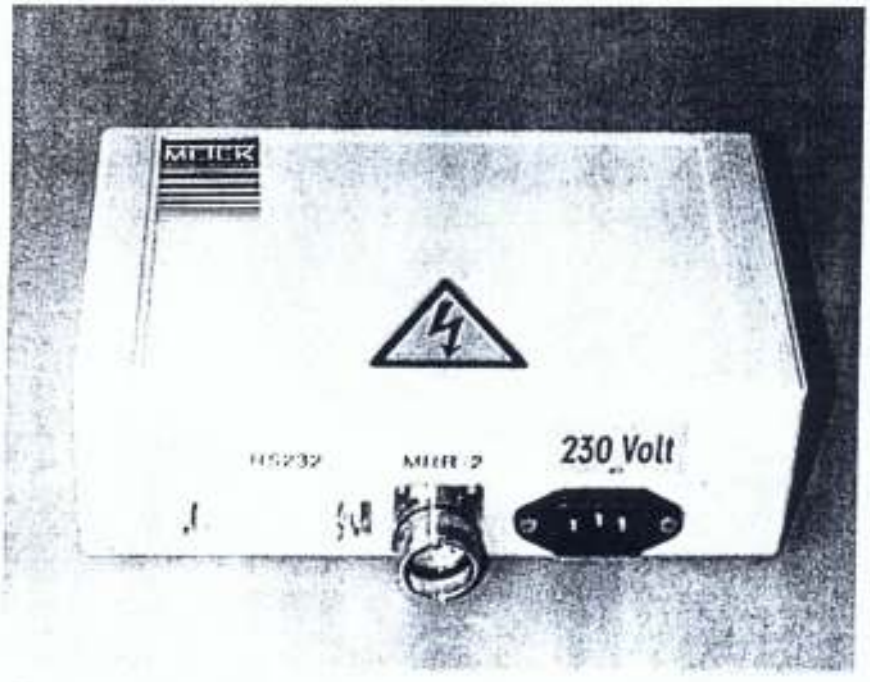

Fig. 3.4: Connection Box

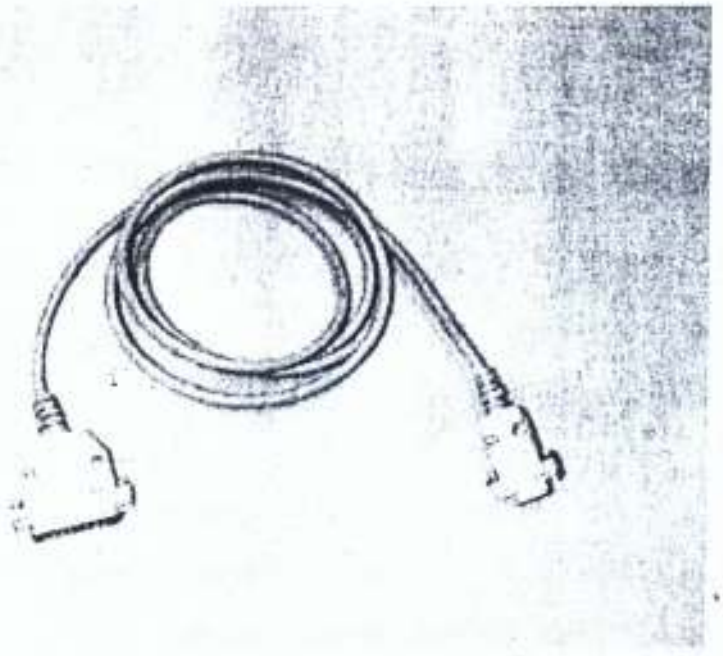

Fig. 3.5: Connecting Cable to the Personal Computer

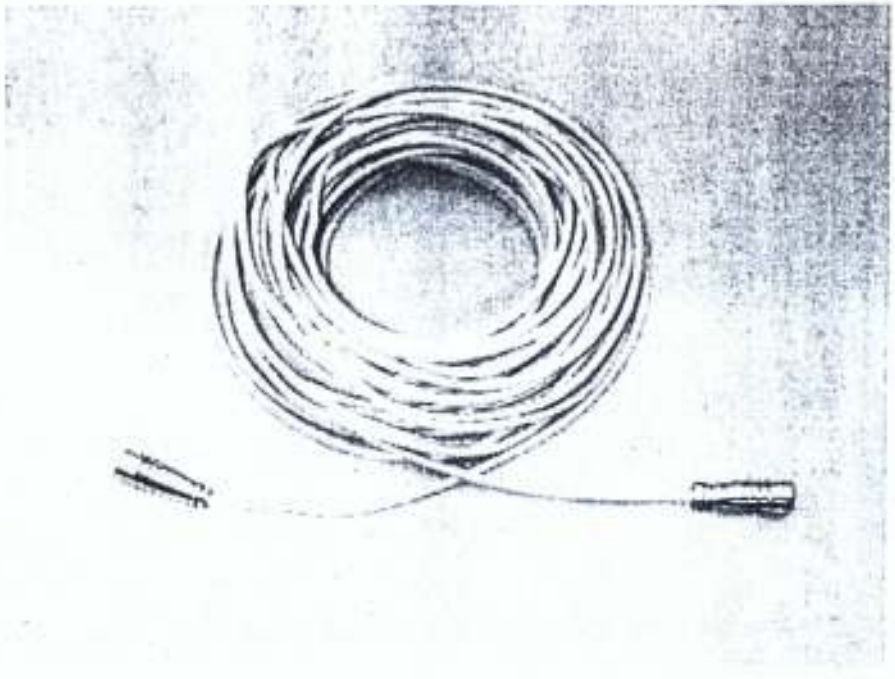

Fig. 3.6: Connection Cable of the RADAR Electronics Unit

Table 3.1: Typical output Data of the Micro Rain Radar.

MRR	0804231020	UTC+01	AVE 60		STP 160 ASL			SMP 125000
H	160	320	480	640	800	960	1120	4800
TF	0.0163	0.053	0.1147	0.1935	0.2845	0.389	0.4956	0.5811
F00	-72.23	-85.21	-81.1	-79.95	-82.58	-80.93	-82.88	-92.71
F01	-74.63	-83.14	-81.22	-79.48	-78.54	-80.69	-79.88	-82.98
F02	-83.65	-85.98	-79.45	-78.6	-77.75	-76.95	-78.65	-78.32
.	.	.	.	.	.	.	.	.
.	.	.	.	.	.	.	.	.
.	.	.	.	.	.	.	.	.
F62	-86.22	-83.91	-79.64	-77.25	-75.78	-75.62	-76.95	-76.64
F63	-75.15	-84.73	-79.66	-77.61	-77.37	-79.07	-78.34	-79.3
N04	6.20E+03	1.10E+05	1.70E+05	3.20E+05	5.00E+05	5.90E+05	3.50E+05	4.00E+05
N05	2.30E+03	3.20E+04	5.30E+04	1.00E+05	1.70E+05	1.90E+05	9.30E+04	1.30E+05
N06	1.10E+03	8.40E+03	2.10E+04	4.00E+04	5.90E+04	7.40E+04	4.20E+04	5.20E+04
.	.	.	.	.	.	.	.	.
.	.	.	.	.	.	.	.	.
.	.	.	.	.	.	.	.	.
N48	0	0	0	0	0	0	0	0.001
N49	0	0	0	0	0	0	0	0.001
Z	36.7	36.7	36.6	36.2	35.3	34.5	33.4	31.4
RR	15.62	18.62	17.65	15.37	11.81	11.15	10.29	7.91
LWC	0.96	1.2	1.12	1.01	0.85	0.87	0.73	0.64

F00–F63: This position represents the spectral reflectivity, the index (00 - 63) stands for the corresponding number of spectral line

N04 – N49: The lines N04-N49 give the drop size distribution (number of drops per volume and class of size) with reference to the height.

CHAPTER FOUR

RESULT AND DISCUSSION

4.1 DROPSIZE DISTRIBUTION

The rain events observed for the years of 2006 and 2008 were analyzed for the 32 different range gates (0-4800 m, with a step of 160 m). Figs. 4.1 and 4.2 show that drop sizes measured varies from 0.25 mm in diameter to about 3.26 mm, with the larger concentration of the diameter around 0.250 - 0.559 mm (with an average diameter interval of 0.04 mm). As the rain drop diameter increases the drop size concentration decreases. Rain drops in the diameter bin of 0.25 mm which represent the drop spectrum N04 contributed most to the rain fall event throughout this period.

4.2 VERTICAL DISTRIBUTION OF RAIN RATE AND LIQUID WATER CONTENT

The variation of the rain rate and liquid water content with height was evaluated and presented in figures (4.3) - (4.6) for the 2-years. The highest rain rate and liquid water content were observed along 0-160 m height for both cases considered. The implication of this is that along this height, we expect to have more attenuation of radio wave due to rainfall compared with the other height bins. This is because wind and hydrodynamic forces are lower at this height than higher height levels.

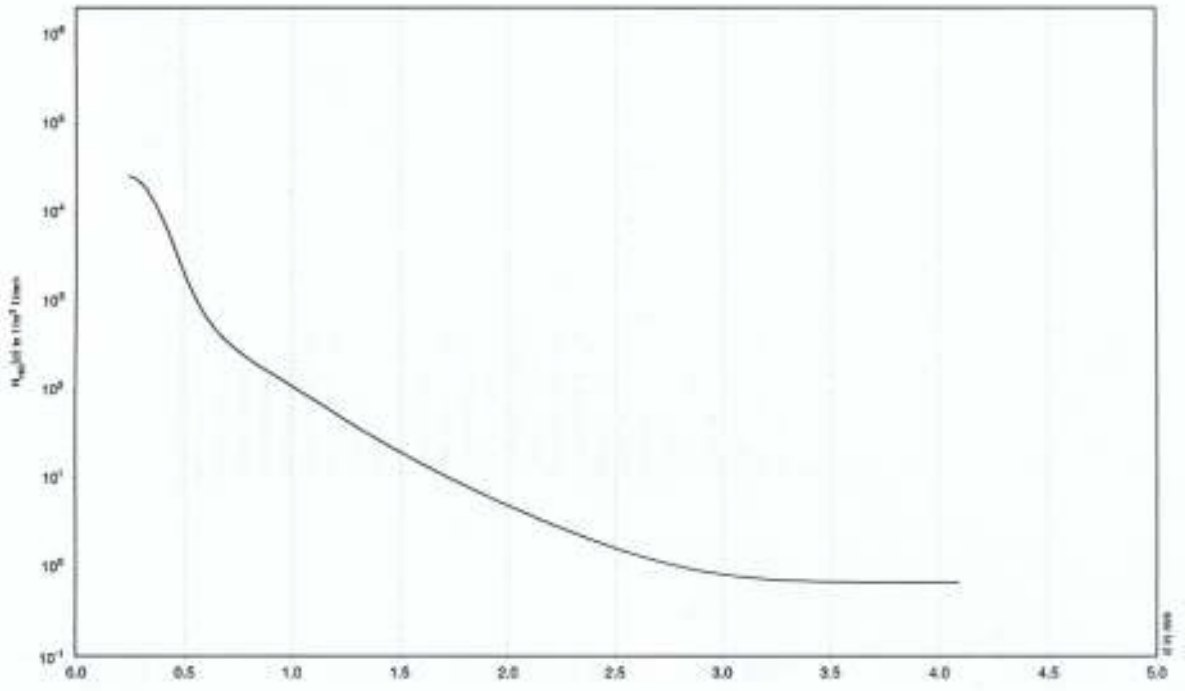

Fig. 4.1: Drop size distribution at height 0-4800 m for the year 2006.

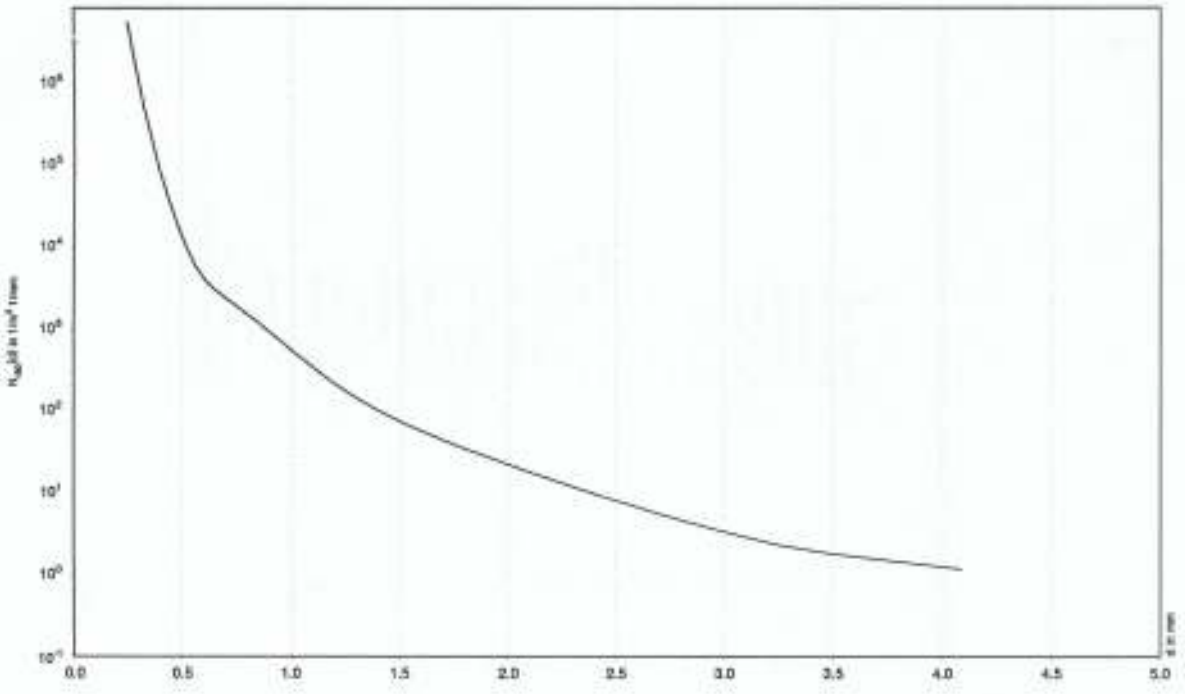

Fig. 4.2: Drop size distribution at height 0-4800 m for the year 2008.

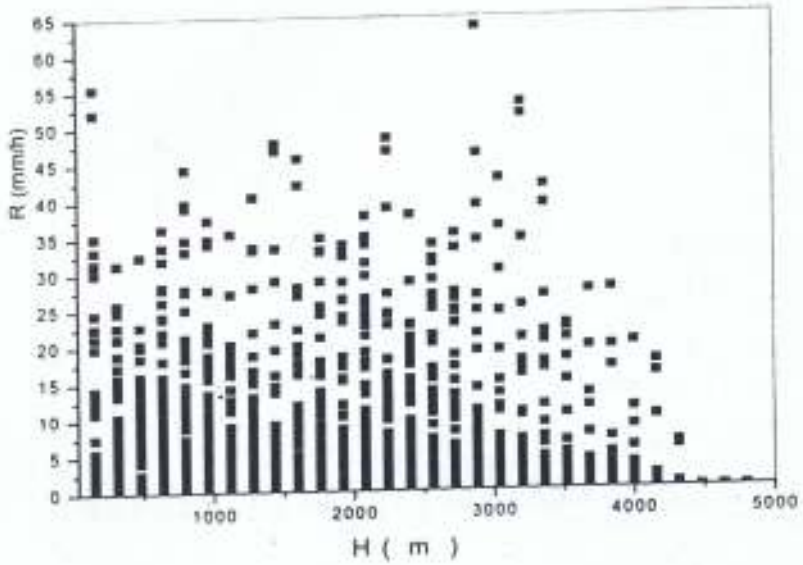

Fig. 4.3: Vertical distribution of rain rate for the year 2006

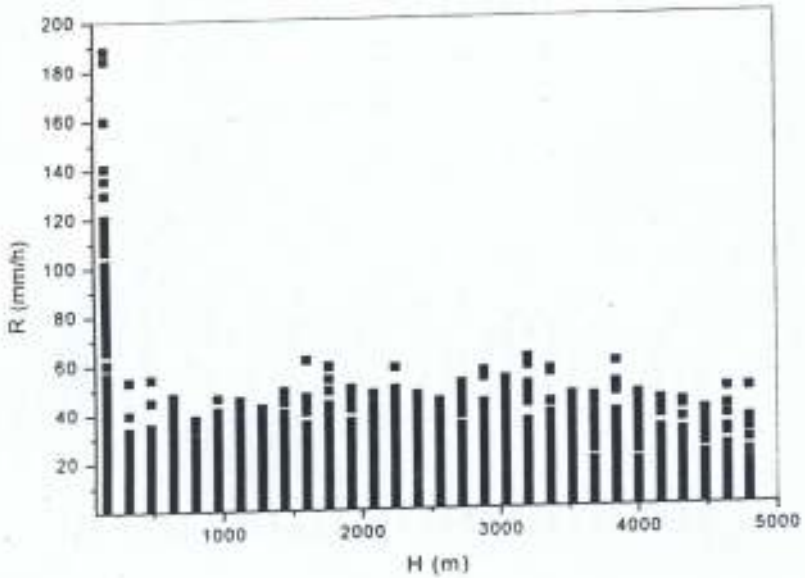

Fig. 4.4: Vertical distribution of rain rate for the year 2008

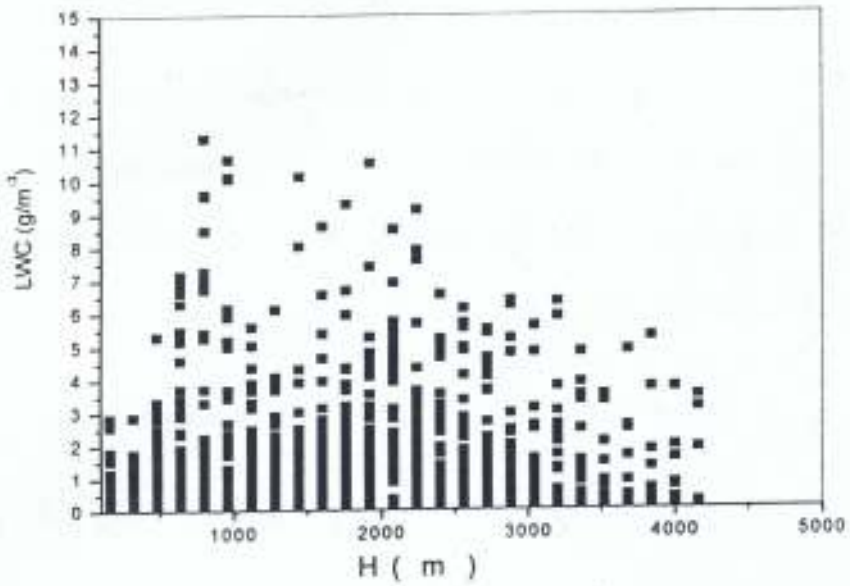

Fig. 4.5: Vertical distribution of liquid water content for the year 2006.

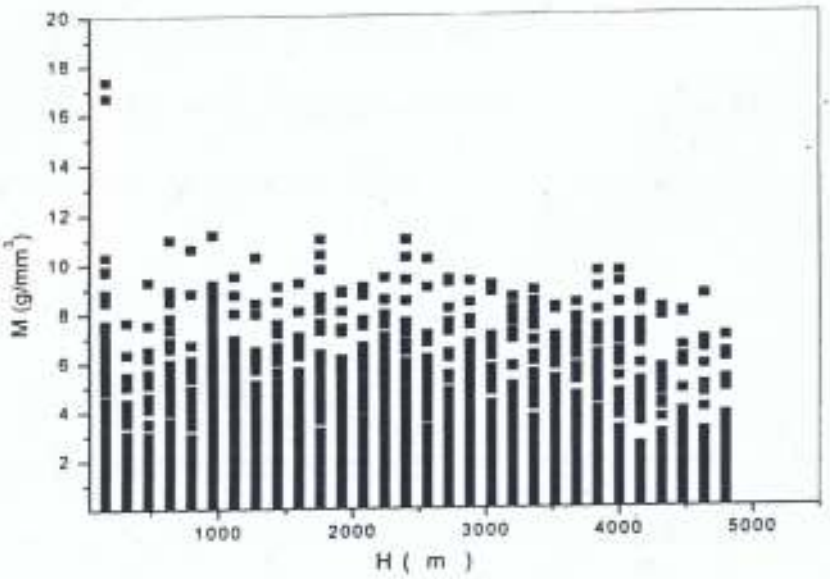

Fig. 4.6: Vertical distribution of liquid water content for the year 2008

4.3 Z – R RELATIONSHIP

All values of R and Z were considered in establishing the general equation for both years of measurement considered (2006 and 2008). This gives two sets of equations, one for each year, the height considered is from 0 – 4800 m above sea level. The data were further divided into units and the heights from 0 – 160 m were also considered for comparison.

The results obtained are

$$Z = 111.66R^{1.17} \text{ (2006)} \quad (4.1)$$

$$Z = 208.5R^{1.21} \text{ (2008)} \quad (4.2)$$

with a correlation coefficients of 0.71 and 0.76 respectively.

Figures (4.7) and (4.8) show the regression lines obtained for the two years considered, as for the height range 0-4800 m. The data was also compared in the height range 0 – 160 m for the two years. The results obtained are shown in figure (4.9) and (4.10) for the regression line. The relevant expressions are shown for the two years as

$$Z = 268.71R^{1.31} \text{ (2006)} \quad (4.3)$$

$$Z = 465.01R^{1.32} \text{ (2008)} \quad (4.4)$$

The correlation coefficients are 0.90 and 0.96 respectively. From equations (4.3) and (4.4), we have good correlation coefficients as compared with those obtained in equations (4.1) and (4.2). This might be associated with the assumption made for the MRR that the measurement is taken in stagnant air, (Metek (2005)).

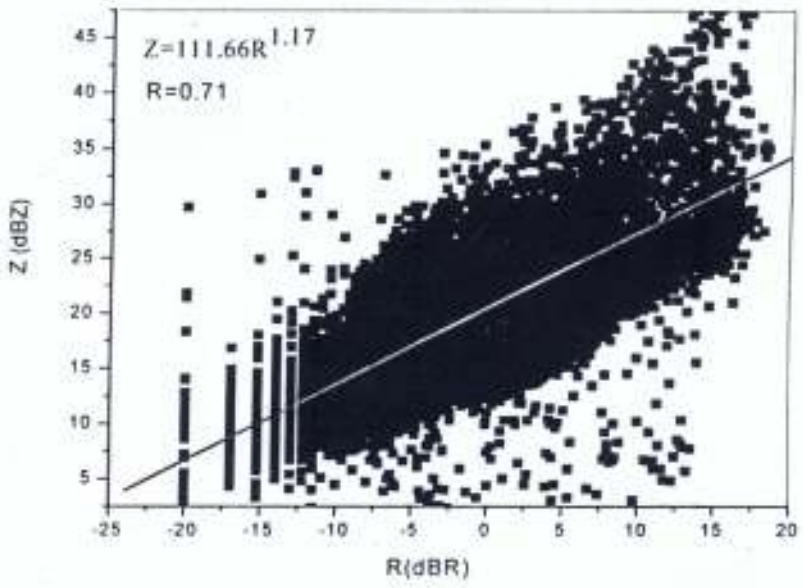

Fig 4.7 - Regression line *Z-R* for the whole data set (at 0-4800 m) for the year 2006

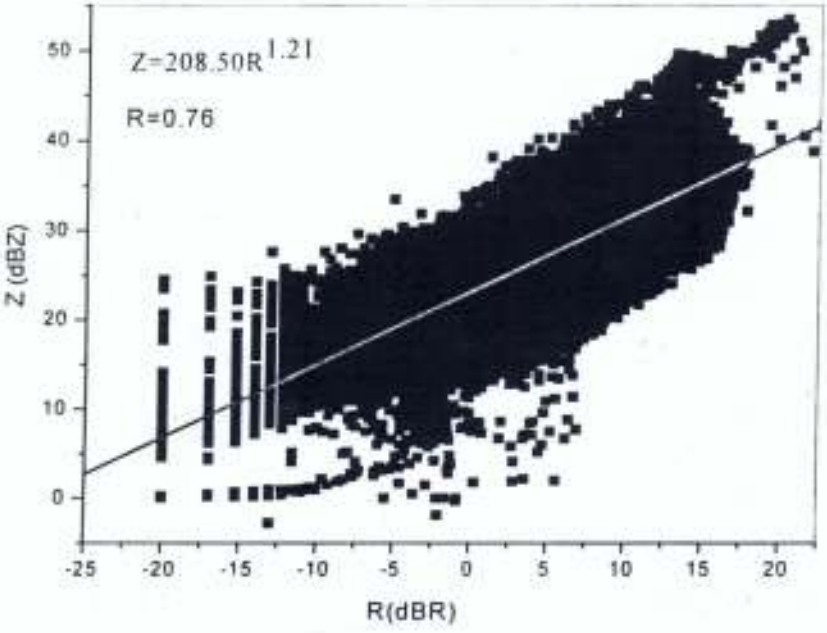

Fig 4.8 - Regression line *Z-R* for the whole data set (at 0-4800 m) for the year 2008

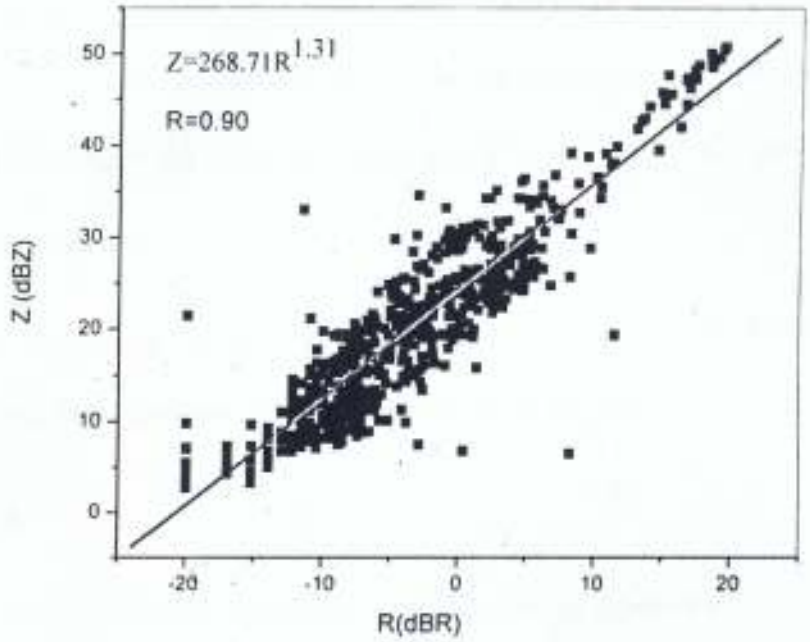

Fig 4.9 - Regression line *Z-R* for the whole data set (at 0-160 m) for the year 2006

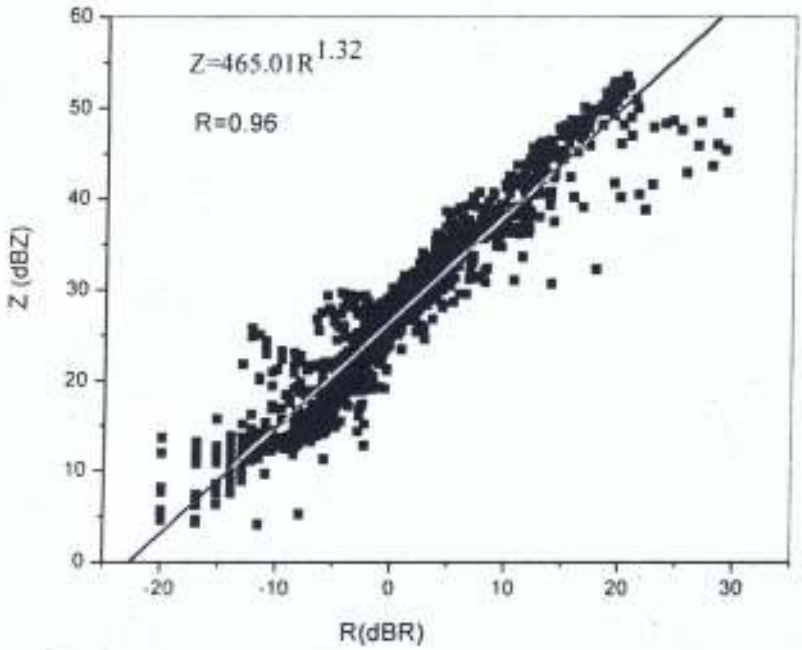

Fig 4.10 - Regression line *Z-R* for the whole data set (at 0-160 m) for the year 2008

4.3.1 Z–R RELATIONSHIP FOR STRATIFORM AND CONVECTIVE RAINFALL

The data were further divided into stratiform and convective rainfall, using the threshold rain rate $R < 50$ mmh^{-1} for stratiform rain and $R \geq 50$ mmh^{-1} for convective rain event as described in Joss et at., (1968).

Figures (4.11) and (4.12) show the regression line for stratiform rainfall while figure (4.13) and figure (4.14) shows that for convective rainfall; the height level in view is from

0 - 4800 m.

The power law results are represented by the following equations

Stratiform rainfall

$Z = 111.25R^{1.17}$ r (0.70) (2006) (4.5)

$Z = 206.99R^{1.20}$ r (0.75) (2008) (4.6)

Convective rainfall

$Z = 64.28R^{1.17}$ r (0.45) (2006) (4.7)

$Z = 90.35R^{1.39}$ r (0.40) (2008) (4.8)

Correlation coefficients of the convective rain type are very low for the height range (0-4800 m) for the year 2008 and 2006 respectively, while for the height range of 0 – 160 m, there is a good correlation above 0.90 for the year 2006 and 2008 respectively. This can be seen in figures (4.15 - 4.18). The values of a and b coefficients for the two years considered and for different rainfall types are given in Table 4.1.

Comparisons were made with other works done at the tropical locations, this is presented in Table 4.2, though these works looked at the vertical profile of the parameters measured and the relationships obtained were based on the vertical profile. This study represents the first of such measurements in Nigeria.

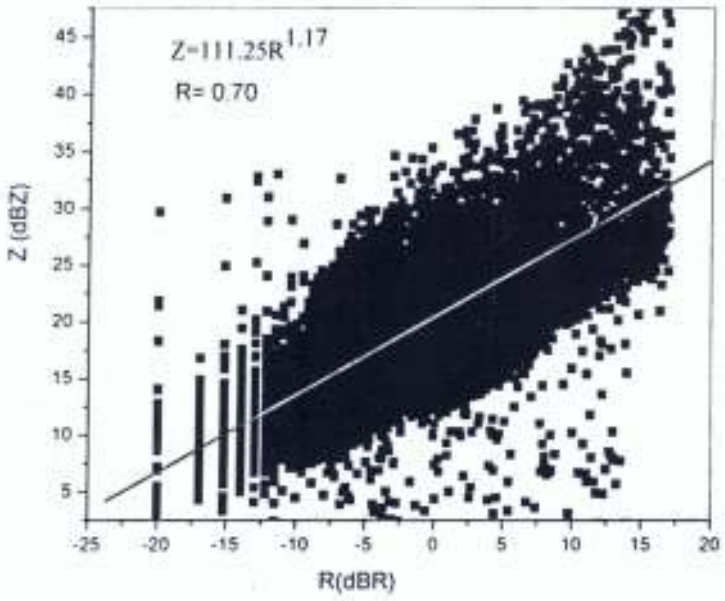

Fig 4.11 - Regression line *Z-R* for Stratiform Rain (at 0-4800 m) for the year 2006

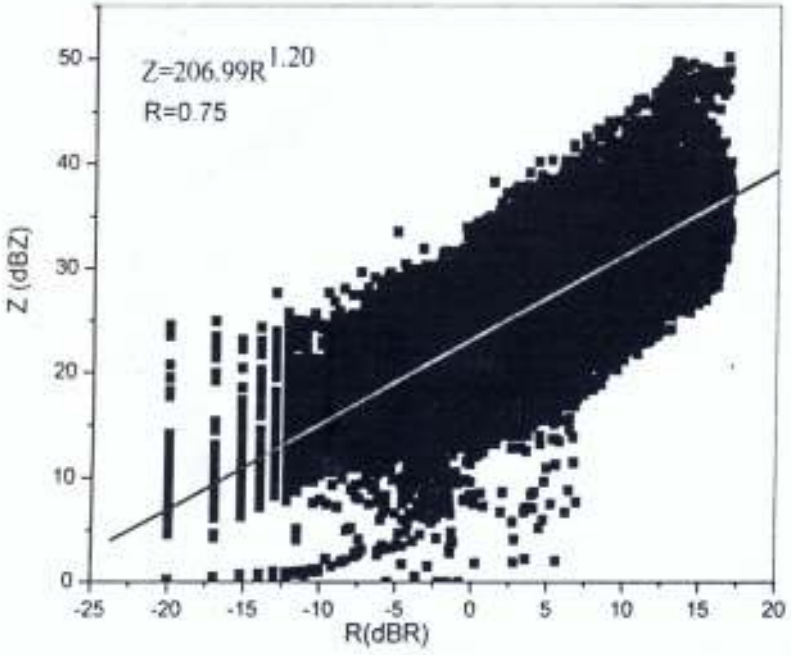

Fig 4.12 - Regression line *Z-R* for Stratiform Rain (at 0-4800 m) for the year 2008

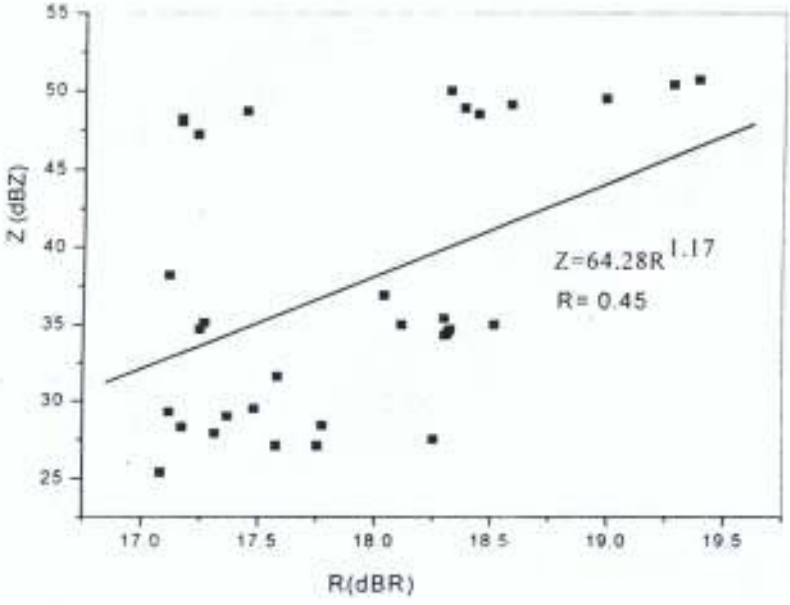

Fig 4.13 - Regression line *Z-R* for Convective Rain (at 0-4800 m) in the year 2006

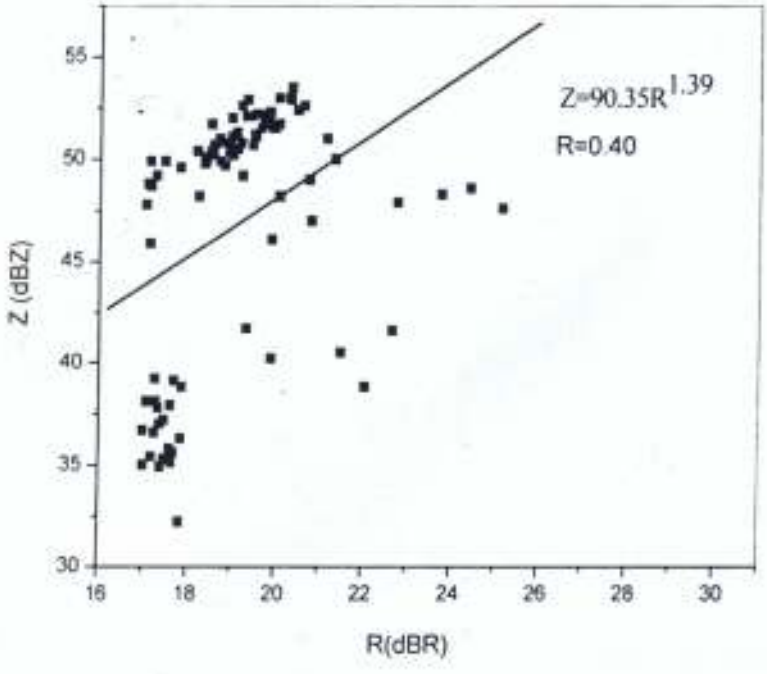

Fig 4.14- Regression line *Z-R* for Convective Rain (at 0-4800 m) in the year 2008

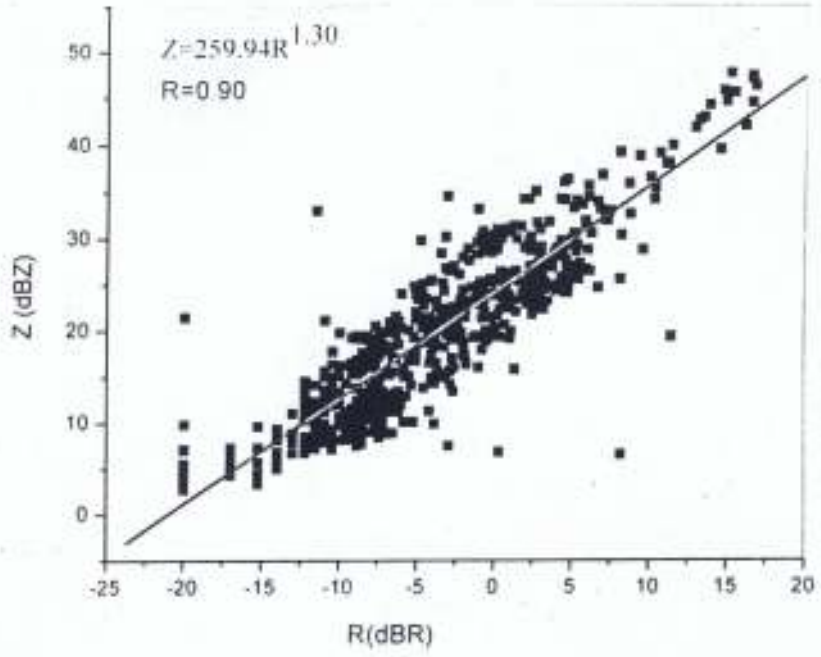

Fig 4.15 - Regression line *Z-R* for Stratiform Rain (at 0-160 m) in the year 2006

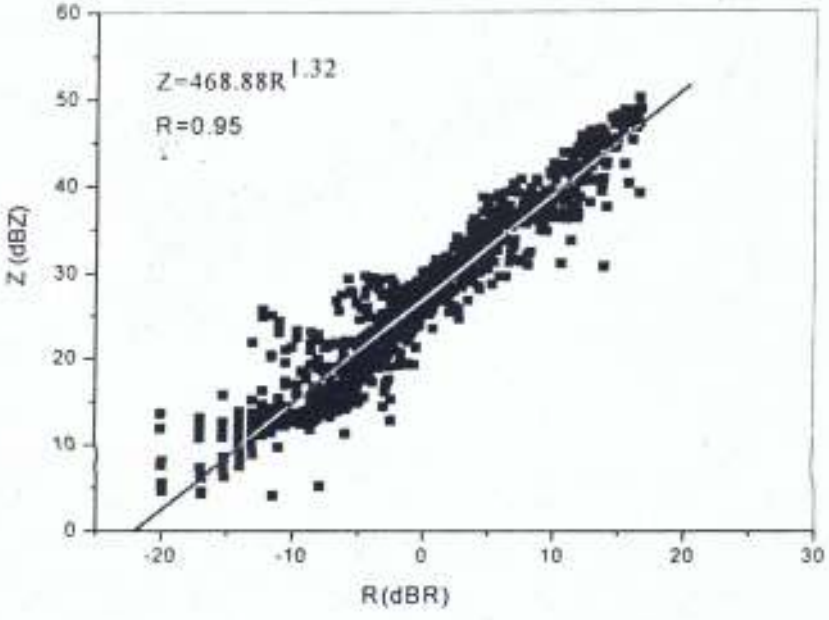

Fig 4.16 - Regression line *Z-R* for Stratiform Rain (at 0-160 m) in the year 2008

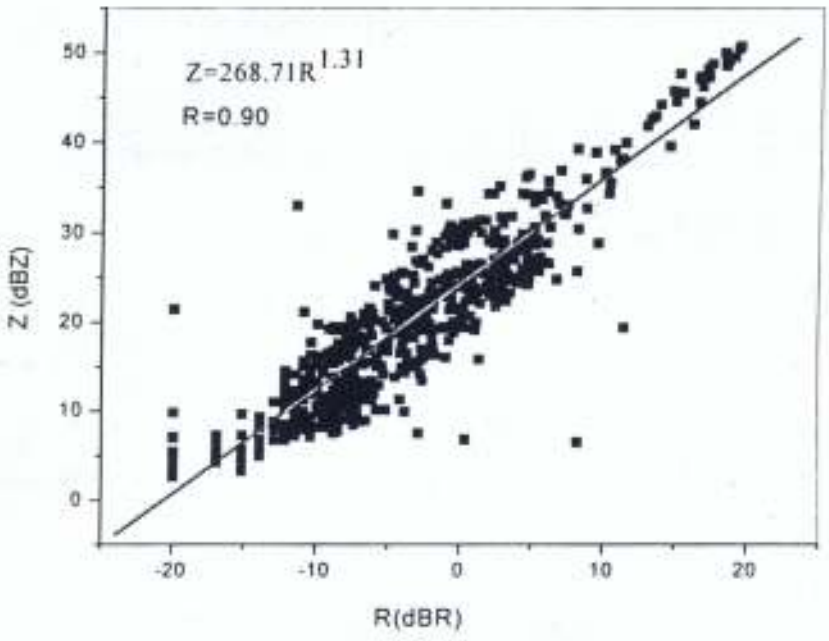

Fig 4.17 - Regression line *Z-R* for Convective Rain (at 0-160 m) in the year 2006

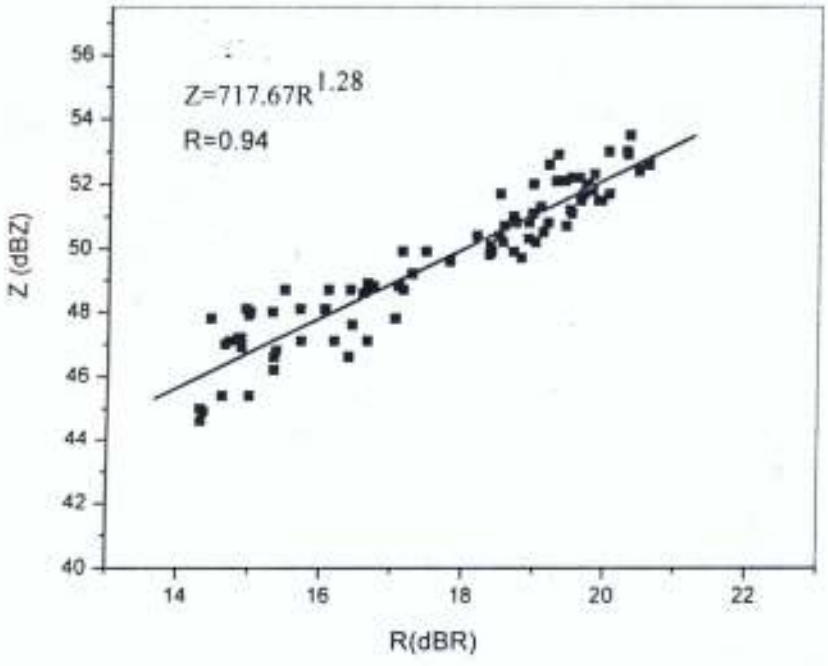

Fig 4.18 - Regression line *Z-R* for Convective Rain (0-160 m) in the year 2008

Table 4.1: Z-R Relationship and correlation coefficients for Convective and Stratiform Rain types in 2008 and 2006 at different heights.

Year	Z-R Relation and correlation coefficients (r)		
	Stratiform	Convective	Height range (metres)
2008	$Z = 206.99R^{1.20}$ $r(0.75)$	$Z = 90.35R^{1.35}$ $r(0.40)$	0-4800
	$Z = 468.88R^{1.32}$ $r(0.95)$	$Z = 717.67R^{1.28}$ $r(0.94)$	0-160
2006	$Z = 111.25R^{1.70}$ $r(0.70)$	$Z = 64.28R^{1.17}$ $r(0.45)$	0-4800
	$Z = 259.94R^{1.30}$ $r(0.90)$	$Z = 268.71R^{1.31}$ $r(0.90)$	0-160

Z is in $mm^6\ m^{-3}$ and R in $mm\ h^{-1}$; r is the coefficient of correlation

Z is in mm^6m^{-3} and R in mmh^{-1}; r is the coefficient of correlation

Table 4.2: Comparison of Z-R Relationships with height at some locations

Rain type	Source	Location	Z-R	r
Stratiform Rain	Joss et al (1970)	Locarno-mouti	$Z = 250R^{1.5}$	
	Marshall and Palmer (1984)	Switzerland	$Z = 220R^{1.6}$	
	CCIR (1982)		$Z = 400R^{1.4}$	
	Fujiwara (1965)	Miami, USA	$Z = 250R^{1.48}$	
	Fundação et al (2004)	Eastern coast, Brazil	$Z = 167.8R^{1.26}$	
	Ajayi and Owolabi (1986)	Ile-Ife, Nigeria	$Z = 312R^{1.35}$	
	Present Study (2008) (0-4800 m) (0-160 m)	Akure, Nigeria	$Z = 206.99R^{1.20}$ $Z = 468.88R^{1.32}$	0.75 0.93
	Present Study (2006) (0-4800 m) (0-160 m)	Akure, Nigeria	$Z = 111.25R^{1.15}$ $Z = 259.94R^{1.30}$	0.70 0.90
Convective Rain	Joss et al (1970)	Locarno - Monti, Austria	$Z = 500R^{1.5}$	
	Jones (1956)	Illinois, USA	$Z = 486R^{1.37}$	
	Fujiwara (1965)	Miami, USA	$Z = 450R^{1.37}$	
	Sekhon and Srivastava (1971)	Cambridge, USA	$Z = 300R^{1.35}$	
	Fundação et al (2004)	Eastern coast, Brazil	$Z = 65.46R^{1.69}$	
	Diem (1966)	Entebbe, Uganda Lwiro, Congo	$Z = 278R^{1.5}$ $Z = 240R^{1.5}$	
	Ajayi and Owolabi (1986)	Ile-Ife, Nigeria	$Z = 524R^{1.37}$	
	Present Study (2008) (0-4800 m) (0-160 m)	Akure, Nigeria	$Z = 90.35R^{1.35}$ $Z = 717.67R^{1.26}$	0.40 0.94
	Present Study (2006) (0-4800 m) (0-160 m)	Akure, Nigeria	$Z = 64.28R^{1.17}$ $Z = 268.71R^{1.31}$	0.45 0.90

Z is in $mm^6\ m^{-3}$ and R in $mm\ h^{-1}$; r is the coefficient of correlation

Z is in mm^6m^{-3} and R in mmh^{-1}; r is the coefficient of correlation

4.4 LIQUID WATER CONTENT

The values of liquid water content (M) and Rain rate (R) for the two years under consideration were plotted and two sets of relationships were obtained,

$$M = 0.106R^{0.98}\ r(0.94) \qquad 2006 \qquad (4.9)$$

$$M = 0.093R^{1.06}\ r(0.94) \qquad 2008 \qquad (4.10)$$

r is the correlation coefficient

Figure 4.19 shows the scattered diagrams and the regression line for M-R for the height 0-4800 m in the year 2006 while figure 4.20 shows that of 0-160 m for same year. Figure 4.21 shows the scattered plots for the height 0-4800 m in the year 2008 while figure 4.22 shows the scattered plots for the height 0-160 m for the same year.

There is a high degree of correlation in all cases considered, the coefficients of correlation are better than 0.91 for most of the rain types. The power relationships obtained were comparable for all the rain types.

Table 4.3 shows the comparison of the M-R relation obtained in Akure with other locations.

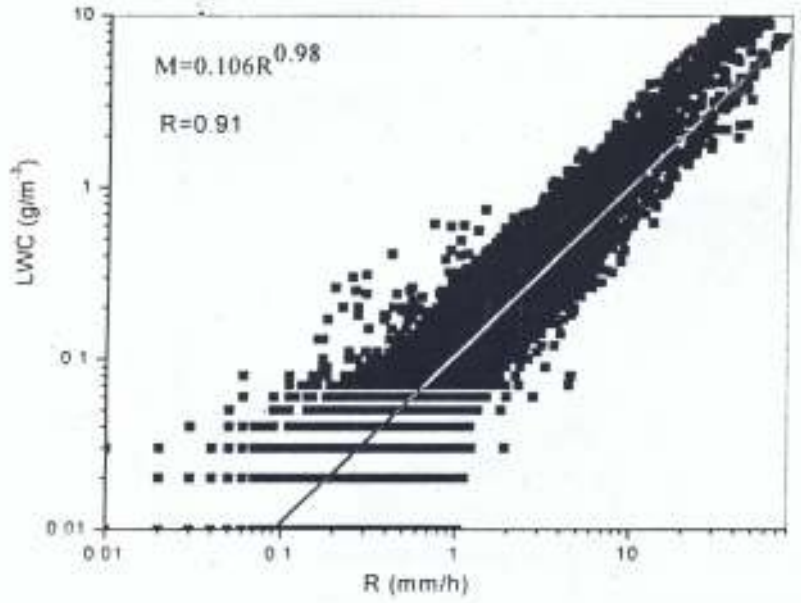

Fig 4.19 - Regression line M-R for the whole data set (at 0-4800 m) for the year 2006

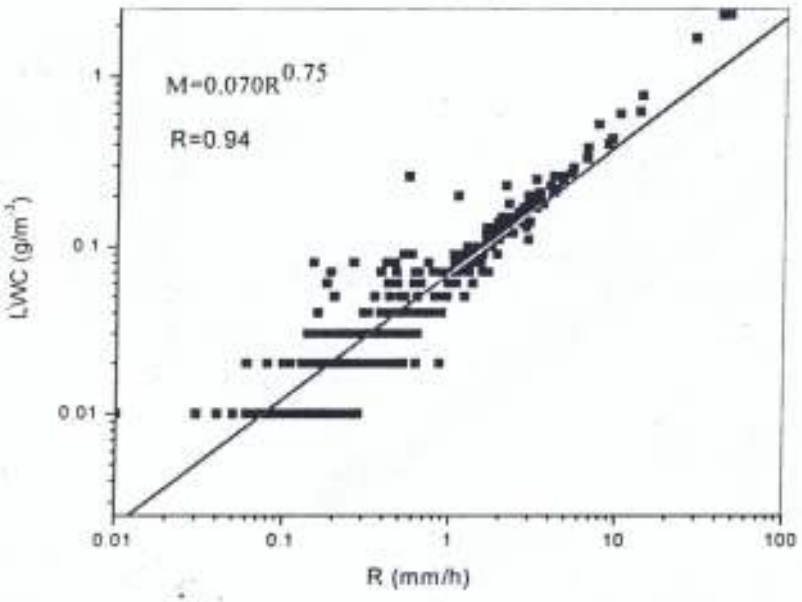

Fig 4.20 - Regression line M-R for the whole data set (at 0-160 m) for the year 2006

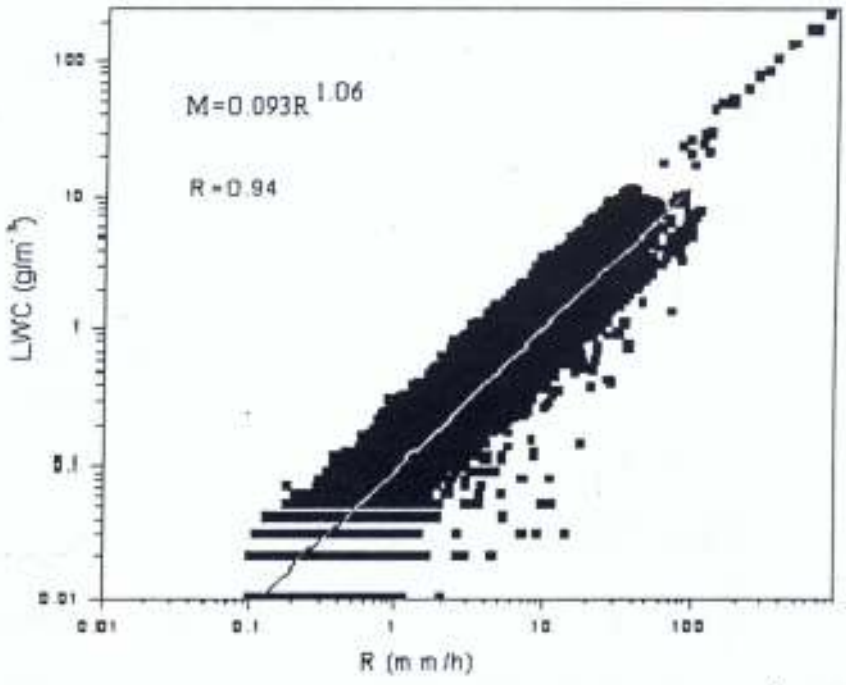

Fig 4.21 - Regression line M-R for the whole data set (at 0-4800 m) for the year 2008

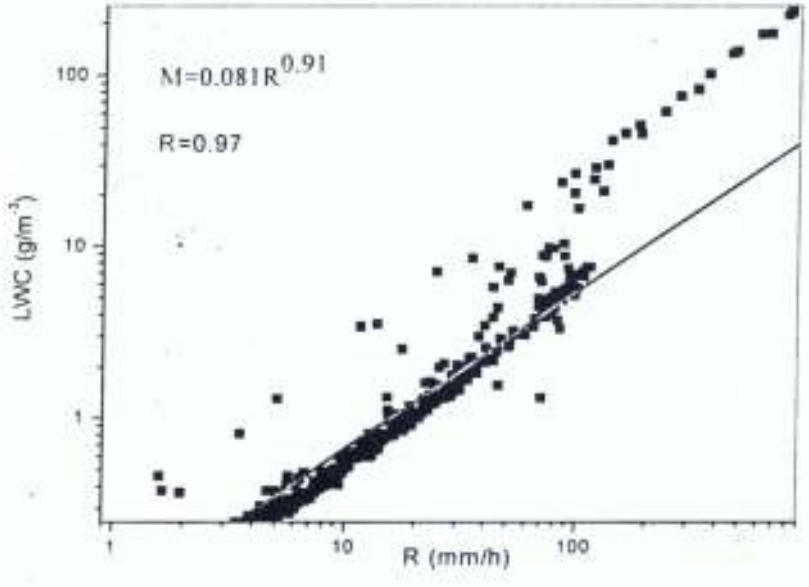

Fig 4.22 - Regression line M-R for the whole data set (at 0-160 m) for the year 2008

Table 4.3: Comparison of M-R relations with height at some locations

Rain Type	Source	Location	M-R
Stratiform Rain	Marshall and Palmer (1984)	Switzerland	$M = 0.072R^{0.88}$
	Ajayi and Owolabi (1986)	Ile-Ife, Nigeria	$M = 0.059R^{0.88}$
	Present Study (2008)	Akure, Nigeria	
	(0-4800 m)		$M = 0.091R^{1.03}$
	(0-160 m)		$M = 0.072R^{0.72}$
	Present Study (2006)		
	(0-4800 m)		$M = 0.101R^{0.93}$
	(0-160 m)		$M = 0.068R^{0.73}$
Convective Rain	Ajayi and Owolabi (1986)	Ile-Ife, Nigeria	$M = 0.063R^{0.89}$
	Sekhon and Srivastava (1971)	Cambridge, USA	$M = 0.052R^{0.94}$
	Jones (1956)	Illinois, USA	$M = 0.052R^{0.97}$
	Mueller (1965)	Miami, USA	$M = 0.053R^{0.92}$
	Present Study (2008)	Akure, Nigeria	
	(0-4800 m)		$M = 0.132R^{0.97}$
	(0-160 m)		$M = 0.020R^{1.52}$
	Present Study (2006)		
	(0-4800 m)		$M = 0.103R^{1.13}$
	(0-160 m)		$M = 0.047R^{1.03}$

The units are M in $g\ m^{-3}$ and R in $mm\ h^{-1}$

M is in gm^{-3} and R in mmh^{-1}.

4.5 SPECIFIC ATTENUATION

The frequency characteristics of specific attenuation for two rain types, stratiform and convective are presented in Figs 4.23 and 4.24 respectively. The specific attenuation was evaluated for frequencies of 1-100 GHz. Tables 4.4 and 4.5, also show the results of the calculation. In general, specific attenuation increases with increasing frequency for stratiform and convective rain types. At a critical frequency, which ranges from 31-100 GHz, the specific attenuation decreased slightly.

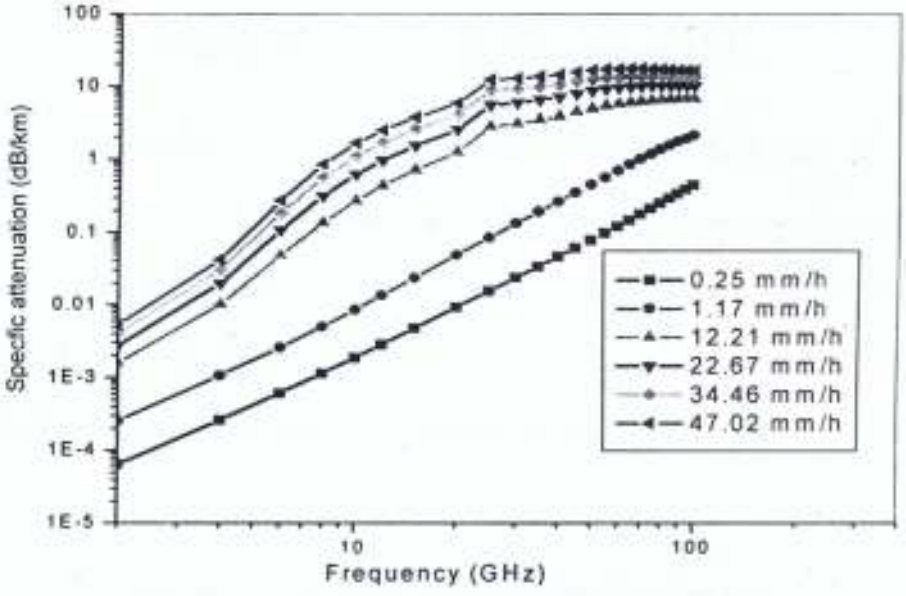

Fig 4.23- Frequency characteristics of specific attenuation for Stratiform rain type at different rain rates

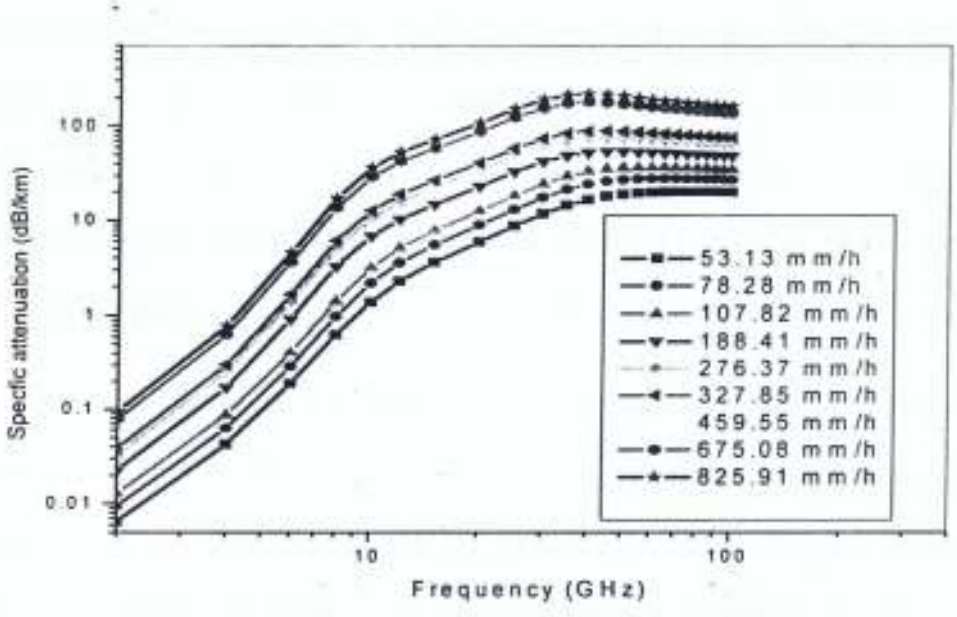

Fig 4.24- Frequency characteristics of specific attenuation for convective rain type at different rain rates

CHAPTER FIVE

CONCLUSIONS AND RECOMMENDATIONS

The rainfall parameters measured for the two years considered have been analyzed for a tropical station, Akure in Nigeria. It was observed that the drop diameters that contributed the most to the rain fall event were in the diameter bin of 0.246 to 0.559 mm (with a diameter interval of 0.04 mm). Rain drops of diameter bin of 0.246 mm contributed the highest number of rain drops to the rain event and this is typical for drop size distribution in the tropical region.

It was also observed that the rain rate below 5 mm/hr contributed the most to the rain event in the height range 0-4800 m while the height range of 0-160 m recorded the highest rain rate.

Empirical relations have been obtained among the rainfall rate, the radar reflectivity factor Z, and liquid water content for the rain types using the least square power law regression. The recorded rainfall rates were classified using the criteria described in Joss et at (1968), for Stratiform rain fall rate $R < 50$mm/h and convective rain $R > 50$ mm/h. These empirical relations have been compared with the results obtained at other locations by other workers. The empirical relations obtained in this analysis are intended to provide useful information about the rainfall parameters in Nigeria for communication purposes.

The correlation coefficients of Z-R relationship for stratiform rainfall for both years and height range considered are good; the values are above 0.70, while that of convective rainfall type is also very good for the height range of 0-160 m with values more than 0.89, but the correlation coefficient for the height range 0-4800 m is poor, with values below 0.50, this might be as a result of the large span of height considered (0-4800 m).

As the communication networks are growing in the country, it is required that extensive research should be done using appropriate parameters and intensive data bank to obtain more data for planning effective communication networks for the nation.

REFERENCES

Adediji, A.T (2003): Calculation of some Propagation characteristics relevant to Earth-Space Communication systems in Nigeria. Unpublished M.Tech. thesis, Federal University of Technology, Akure Nigeria.

Adimula, I.A and Ajayi, G.O (1996): Variations in raindrop size distribution and specific attenuation due to rain in Nigeria. Ann. Telecomm. vol. **51**, no 1-2, pp 87-93.

Ajayi, G.O and Olsen, R.L (1985): Modeling of a Tropical raindrop size distribution for microwave and millimeter wave applications, *Radio Sci.*, vol. **20**, pp. 193-202.

Ajayi, G.O (1984): Raindrop size characteristics during a Tropical Thunderstorm and Monsoon rainfall at Ile- Ife. Extrait Annales des Telecommunication, tome **39**. pp 515-521.

Ajayi, G.O, and Owolabi, I.E (1987): Rainfall Parameters from disdrometer dropsize measurements at a Tropical station. Annales des Telecommunication, tome **42**. pp 1-10.

Ajewole, M.O, Kolawole, L.B and Ajayi, G.O (1999): Theoretical study of the effect of different types of Tropical rainfall on microwave and millimeter-wave Propagation. Radio science, volume **34**, Number 5, pp 1103-1124.

Ajewole, M.O (1997): Scattering and attenuation of centimeter and millimeter Radio signal by Tropical rainfall. Unpublished Ph.D Thesis, Federal University of Technology, Akure Nigeria.

America Meteorological Society Glossary, (2007): Radar constant, retrieved on July, 2007, f rom *http://amsglossary.allenpress.com/glossary/search?p=1&query=radar+constant&submit=Search.*

America Meteorological Society Glossary, (2007): Rainfall Rate, retrieved on July, 2007, from *http://amsglossary.allenpress.com/glossary/search?p=1&query=rainfall+rate&submit=Search.*

America Meteorological Society Glossary, (2007): Rainfall Rate, retrieved on July, 2007, from *http://amsglossary.allenpress.com/glossary/search?p=1&query=radar+reflectivity&submit=Search.*

Atlas, D., Srivastava, R. and Sekhon, R. (1973): Doppler radar characteristics of Precipitation at vertical incidence, Rev. Geophys. Space phys., **11**, pp 1-35.

Battan, L.J (1973): Radar observation of the Atmosphere. The University of Chicago Press.

C.C.I.R. Report 882 (1982): Propagation in non-ionized media: Scattering by precipitation. C.C.I.R. XVth Plenary Assembly, Study Group V, International Telecommunication Union, Geneva.

Campistron, B.,G. Despaux, and J. P., Lacaux, (1987): A Microcomputer Data- Acquisition system for real-time Processing of raindrop size distribution Measured with the RD69 distrometer. J. *Atmos. Oceanic Technol.* **4**. pp 536-540.

Collier, C.G., (1989): Application of Weather radar systems. A guide to uses of radar data in Meteorology and Hydrology. Ellis Horwoods Cluchester, UK. pp 294.

Curtis, D.C., (1999): Comparing spatial distribution of rainfall derived from rain gages and radar. Journal of Flood plain Management. Brett S. Clyde NEXRAIN Corporation, Folsom, CA.

Diederich M., Crewell S., Simmer C., and Uijlenhoet R. (2004): Investigation of rainfall microstructure and variability using vertically pointing radar and disdrometer. Proceedings of ERAD (2004): pp 80–86

Deirmendjan, D. (1969): Electromagnetic scattering on spherical polydispersion. New York Elsevier, pp 75-119.

Sempere T,D., Porrà, J.M. and Creutin, J.D (1994): A general formulation for raindrop size distribution. *J. Appl. Meteorol.*, **33**, pp 1494–1502.

Sempere T,D., Porra, J.M and Creutin, J.D (1998): Experimental evidence of a general description for raindrop size distributions. J. Appl. Meteorol. **32**, pp 284-296.

Strauch. R.G (1976): Theory and application of the FM-CW doppler radar. Ph.D. Thesis, Elecrical Engineering, University of Colorado, pp 97.

Uijlenhoet, R. and Stricker, J.N.M. (1999): A conatstent rainfall parameterisation based on the exponential raindrop size distribution. J. Hydrology **218**, pp 101-127.

Ulbrich, C.W., Lee, L.G., 1999: Rainfall measurement Error by WSR-88D radars due to variations in Z–R Law Parameters and the radar constant. Journal of Atmospheric and Oceanic Technology, **16**, pp 1017-1024.

Wei - Zhang and Nader, M. IEEE 802.16 Broadband wireless access working group 2000, Recommendation: Power-Law Parameters of rain specific attenuation.

Appendix

Tables 4.4 – 4.6

Table 4.4- specific attenuation due to strati-form rain at some rain rate.

Frequency (GHz)	0.25 mm/h	1.17 mm/h	12.21 mm/h	22.67 mm/h	34.46 mm/h	47.02 mm/h
1	1.652E-07	6.558E-07	0.00036	0.0006148	0.000882	0.001154
2	6.397E-05	0.0002556	0.001574	0.0027527	0.004019	0.005322
4	0.0002597	0.001063	0.010112	0.0194895	0.030384	0.042244
6	0.000607	0.0025712	0.047787	0.1066449	0.1836	0.274767
8	0.0011299	0.0049768	0.13516	0.3140326	0.555579	0.848448
10	0.0018552	0.0084992	0.27	0.6195668	1.086936	1.649569
12	0.0028088	0.01336	0.435344	0.970765	1.670358	2.498775
15	0.0046904	0.0234389	0.716995	1.5328406	2.563348	3.754343
20	0.0091486	0.0485916	1.247651	2.5427317	4.116736	5.886354
25	0.0153674	0.084702	2.802157	5.541653	8.791302	12.3819
30	0.0234711	0.1320912	3.069649	5.9200449	9.233263	12.84132
35	0.0335613	0.1909581	3.459964	6.5072455	9.978005	13.70309
40	0.0457892	0.262267	3.851805	7.059657	10.63767	14.42092
45	0.0603212	0.347106	4.436931	7.9254245	11.73599	15.7055
50	0.0773397	0.4466864	4.945232	8.617951	12.55003	16.58791
55	0.0970945	0.5619091	5.371005	9.1469406	13.11449	17.13473
60	0.1198811	0.6932458	5.71678	9.532525	13.47355	17.41829
65	0.1460792	0.8405819	5.992557	9.8049487	13.68215	17.52055
70	0.1760086	1.002386	6.20696	9.9856326	13.77589	17.49156
75	0.2099775	1.1766201	6.371406	10.099089	13.79309	17.38326
80	0.2481849	1.3601515	6.492801	10.158013	13.75152	17.2176
85	0.2907474	1.5492782	6.581069	10.179545	13.6749	17.02404
90	0.3375244	1.7401048	6.642325	10.173075	13.57495	16.81579
95	0.3881741	1.9287588	6.682187	10.146478	13.46088	16.60261
100	0.4422697	2.1114421	6.706243	10.107672	13.34218	16.39495

Table 4.5- specific attenuation due to convective-form rain at some rain rate.

Frequency (GHz)	53.13 mm/h	78.28 mm/h	107.82 mm/h	188.41 mm/h	276.37 mm/h	327.85 mm/h	459.55 mm/h	675.08 mm/h	825.91 mm/h
1	0.001443	0.002074	0.002799	0.004728	0.006823	0.008036	0.011105	0.016051	0.019471
2	0.006453	0.009357	0.01272	0.022401	0.032591	0.03852	0.053606	0.078101	0.09514
4	0.042361	0.062894	0.087179	0.171094	0.25392	0.302792	0.42882	0.63737	0.784585
6	0.19037	0.289182	0.408486	0.920207	1.38969	1.670092	2.401839	3.632956	4.513292
8	0.627508	0.975569	1.404684	3.25624	5.014387	6.078776	8.893743	13.71836	17.21842
10	1.379044	2.159472	3.127912	6.814285	10.51889	12.76544	18.71664	28.93996	36.36978
12	2.267048	3.531627	5.093526	10.28484	15.75384	19.05256	27.74491	42.56762	53.27863
15	3.585178	5.504868	7.845201	14.78209	22.32038	26.82219	38.56906	58.32952	72.45807
20	5.910719	8.930131	12.55789	22.9673	34.27554	40.97386	58.31282	87.15705	107.6022
25	8.728871	13.10485	18.33262	32.93835	48.94924	58.40533	82.8126	123.253	151.8283
30	11.75661	17.54204	24.41527	42.11861	62.18556	73.98352	104.3003	154.2224	189.3276
35	14.46882	21.38573	29.53336	48.78282	71.3383	84.51106	118.1402	173.0152	211.3299
40	16.57753	24.20992	33.10333	52.25627	75.53867	89.0266	123.1899	178.3271	216.4957
45	18.02504	25.98432	35.15049	53.52724	76.49168	89.68899	122.8555	175.803	212.1441
50	18.95948	26.99243	36.13971	53.57183	75.77338	88.44095	120.0545	170.0333	204.0758
55	19.51912	27.47967	36.4532	53.09448	74.46218	86.58161	116.6527	163.8107	195.7293
60	19.85065	27.68124	36.43252	52.42663	73.02585	84.65372	113.3718	158.1173	188.2495
65	20.03848	27.72419	36.25266	51.78725	71.75762	82.98911	110.6294	153.4818	182.2265
70	20.12999	27.6722	35.99287	51.15498	70.59156	81.49146	108.2412	149.5518	177.1778
75	20.17099	27.58601	35.72829	50.59368	69.598	80.23203	106.2736	146.371	173.1229
80	20.15549	27.44861	35.42649	50.06898	68.70753	79.11896	104.573	143.6747	169.7146
85	20.11782	27.30404	35.14075	49.56	67.87634	78.09375	103.0404	141.2916	166.728
90	20.14591	27.26703	35.01344	49.10268	67.14701	77.20187	101.7261	139.275	164.2159
95	19.98218	26.98261	34.58171	48.6627	66.46381	76.37461	100.5274	137.4645	161.9766
100	19.89537	26.81441	34.31228	48.24952	65.83388	75.61715	99.44302	135.8458	159.9854

Table 4.6: Typical output Data of the Micro Rain Radar for one minute.

MRR	804231020	UTC+01	AVE 60		STP 160 ASL			SMP 125000
H	160	320	480	640	800	960	1120	4800
TF	0.0163	0.053	0.1147	0.1935	0.2845	0.389	0.4956	.....-0.5811
F00	-72.23	-85.21	-81.1	-79.95	-82.58	-80.93	-82.88	.....-92.71
F01	-74.63	-83.14	-81.22	-79.48	-78.54	-80.69	-79.88	.....-82.98
F02	-83.65	-85.98	-79.45	-78.6	-77.75	-76.95	-78.65	.....-78.32
F03	-82.6	-79.76	-78.46	-77.49	-76.73	-78.51	-78.42	.....-80.79
F04	-94.35	-82.34	-81.15	-79.24	-77.48	-77.11	-79.75	.....-79.4
F05	-94.73	-83.87	-82.15	-80.1	-78.04	-78.03	-81.61	.....-80.35
F06	-94.35	-86.18	-82.62	-80.67	-79.19	-78.79	-81.74	.....-81.02
F07	-86.17	-84.65	-82.71	-81.67	-80.38	-79.67	-82.35	.....-82.11
F08	-82.35	-82.28	-82.2	-81.86	-80.7	-79.99	-83.83	.....-83.85
F09	-79.51	-79.94	-81.62	-81.78	-80.84	-79.76	-85.36	.....-86.58
F10	-77.03	-77.58	-81.11	-82.42	-81.85	-80.1	-86.64	.....-88.13
F11	-74.91	-75.42	-79.36	-82.29	-83.13	-80.64	-85.67	.....-85.79
F12	-73.16	-73.51	-76.8	-79.82	-83.29	-81.34	-85.08	.....-83.85

Table 4.6 Continues

F13	-71.39	-71.41	-74.27	-77.08	-82.98	-82.98	-86.08	.....-82.78
F14	-69.38	-69.33	-72.29	-75.41	-82.94	-84.85	-83.2	.....-80.25
F15	-67.37	-67.5	-70.79	-74.51	-82.86	-84.38	-79.22	.....-77.19
F16	-65.89	-66.1	-69.46	-73.29	-81.41	-82.02	-76.6	.....-74.95
F17	-64.89	-64.9	-67.85	-71.43	-78.65	-79.4	-74.83	.....-73.45
F18	-64.04	-63.73	-66.07	-69.32	-76.14	-77.03	-73.35	.....-72.37
F19	-63.08	-62.59	-64.32	-67.15	-73.74	-74.4	-71.62	.....-71.25
F20	-61.89	-61.35	-62.68	-65.16	-70.94	-71.4	-69.27	.....-69.29
F21	-60.42	-59.84	-61.13	-63.57	-68.3	-68.3	-66.47	.....-66.67
F22	-59.06	-58.34	-59.75	-62.19	-65.99	-65.55	-63.67	.....-64.25
F23	-58.19	-57.39	-58.52	-60.57	-63.63	-63.27	-61.39	.....-62.33
F24	-57.49	-56.77	-57.64	-59.17	-61.47	-61.37	-59.9	.....-61.02
F25	-56.56	-55.91	-56.66	-57.87	-59.91	-59.93	-59.1	.....-60.37
F26	-55.6	-54.97	-55.65	-56.67	-58.57	-58.78	-58.61	.....-60.21
F27	-54.91	-54.32	-55.07	-55.92	-57.3	-57.86	-58.29	.....-60.34
F28	-54.32	-53.84	-54.55	-55.4	-56.37	-57.23	-58.32	.....-60.82
F29	-53.93	-53.65	-54.13	-55.07	-55.9	-56.94	-58.64	.....-61.63
F30	-53.71	-53.6	-53.84	-54.9	-55.7	-56.71	-59	.....-62.58
F31	-53.47	-53.63	-53.69	-54.58	-55.43	-56.5	-59.33	.....-63.24

Table 4.6 Continues

F32	-53.23	-53.86	-53.76	-54.18	-55.13	-56.76	-60.09	.....-63.91
F33	-53.25	-54.16	-53.94	-54.09	-55.09	-57.32	-61.05	.....-64.66
F34	-53.6	-54.86	-54.5	-54.62	-55.55	-58	-62.1	.....-65.64
F35	-53.96	-55.93	-55.56	-55.66	-56.59	-59.16	-63.45	.....-67.27
F36	-54.17	-56.92	-56.96	-57	-58.1	-61.04	-65.39	.....-69.28
F37	-54.29	-57.8	-58.54	-58.69	-60.02	-63.3	-67.82	.....-71.61
F38	-54.52	-58.82	-60.33	-60.59	-62.07	-65.48	-70.54	.....-74.44
F39	-55.01	-59.95	-62.58	-62.8	-64.33	-67.95	-73.64	.....-77.34
F60	-82.17	-78.98	-78.13	-76.25	-74.57	-75.76	-76.64	.....-77.91
F61	-81.62	-78.93	-77.4	-75.79	-74.82	-76.1	-76.25	.....-77.21
F62	-86.22	-83.91	-79.64	-77.25	-75.78	-75.62	-76.95	.....-76.64
F63	-75.15	-84.73	-79.66	-77.61	-77.37	-79.07	-78.34	.....-79.3

Table 4.6 Continues

N04	6.20E+03	1.10E+05	1.70E+05	3.20E+05	5.00E+05	5.90E+05	3.50E+05	.....4.00E+05
N05	2.30E+03	3.20E+04	5.30E+04	1.00E+05	1.70E+05	1.90E+05	9.30E+04	.....1.30E+05
N06	1.10E+03	8.40E+03	2.10E+04	4.00E+04	5.90E+04	7.40E+04	4.20E+04	.....5.20E+04
N07	3.50E+03	5.90E+03	1.00E+04	1.60E+04	2.20E+04	3.00E+04	1.80E+04	.....2.00E+04
N08	4.30E+03	5.20E+03	6.00E+03	7.80E+03	1.10E+04	1.40E+04	6.70E+03	.....7.00E+03
N09	4.50E+03	4.90E+03	3.80E+03	4.20E+03	5.50E+03	8.20E+03	2.70E+03	.....2.10E+03
N10	4.40E+03	4.70E+03	2.50E+03	2.00E+03	2.40E+03	4.40E+03	1.20E+03	.....8.90E+02
N11	4.20E+03	4.50E+03	2.20E+03	1.30E+03	1.10E+03	2.30E+03	8.70E+02	.....8.50E+02
N12	3.80E+03	4.10E+03	2.40E+03	1.50E+03	6.60E+02	1.20E+03	5.50E+02	.....7.40E+02
N13	3.50E+03	4.10E+03	2.60E+03	1.70E+03	4.70E+02	4.80E+02	2.70E+02	.....5.80E+02
N14	3.50E+03	4.20E+03	2.60E+03	1.60E+03	3.10E+02	2.00E+02	3.30E+02	.....6.80E+02
N15	3.50E+03	4.10E+03	2.40E+03	1.20E+03	2.00E+02	1.40E+02	5.30E+02	.....8.90E+02
N16	3.20E+03	3.70E+03	2.10E+03	1.10E+03	1.90E+02	1.70E+02	6.40E+02	.....9.80E+02
N17	2.70E+03	3.20E+03	2.00E+03	1.10E+03	2.30E+02	2.10E+02	6.30E+02	.....9.00E+02
N18	2.20E+03	2.80E+03	2.00E+03	1.20E+03	2.80E+02	2.50E+02	5.80E+02	.....7.80E+02
N19	1.80E+03	2.40E+03	2.00E+03	1.30E+03	3.40E+02	3.10E+02	5.90E+02	.....7.10E+02
N20	1.60E+03	2.20E+03	2.00E+03	1.40E+03	4.50E+02	4.20E+02	7.10E+02	.....8.00E+02
N21	1.60E+03	2.20E+03	2.00E+03	1.40E+03	5.70E+02	6.00E+02	9.40E+02	.....1.00E+03

Table 4.6 Continues

N22	1.50E+03	2.10E+03	1.80E+03	1.30E+03	6.60E+02	7.60E+02	1.20E+03	.....1.30E+03
N23	1.20E+03	1.80E+03	1.70E+03	1.30E+03	7.60E+02	8.50E+02	1.40E+03	.....1.40E+03
N24	1.00E+03	1.40E+03	1.40E+03	1.20E+03	8.30E+02	9.00E+02	1.40E+03	.....1.30E+03
N25	8.60E+02	1.20E+03	1.20E+03	1.10E+03	7.90E+02	8.80E+02	1.30E+03	.....1.00E+03
N26	7.30E+02	1.00E+03	1.00E+03	9.80E+02	7.30E+02	7.90E+02	9.80E+02	.....7.30E+02
N27	5.90E+02	8.10E+02	8.20E+02	8.00E+02	6.80E+02	6.80E+02	7.30E+02	.....4.90E+02
N28	4.60E+02	6.20E+02	6.30E+02	6.20E+02	5.70E+02	5.40E+02	5.00E+02	.....3.00E+02
N29	3.40E+02	4.40E+02	4.80E+02	4.60E+02	4.30E+02	4.20E+02	3.20E+02	.....1.70E+02
N30	2.40E+02	3.00E+02	3.40E+02	3.20E+02	3.10E+02	3.00E+02	2.00E+02	.....9.50E+01
N31	1.70E+02	2.00E+02	2.40E+02	2.30E+02	2.20E+02	2.20E+02	1.30E+02	.....5.60E+01
N32	1.20E+02	1.20E+02	1.50E+02	1.70E+02	1.60E+02	1.30E+02	7.10E+01	.....3.30E+01
N33	7.80E+01	7.60E+01	9.80E+01	1.10E+02	1.00E+02	7.80E+01	3.80E+01	.....1.90E+01
N34	4.70E+01	4.30E+01	5.60E+01	6.40E+01	6.70E+01	4.40E+01	2.00E+01	.....9.758
N35	2.80E+01	2.20E+01	2.90E+01	3.30E+01	3.40E+01	2.20E+01	9.459	.....4.44
N36	1.70E+01	1.10E+01	1.40E+01	1.60E+01	1.60E+01	9.345	3.978	.....1.833
N37	1.10E+01	6.045	6.164	7.043	6.629	3.647	1.493	.....0.701
N38	6.86	3.126	2.682	2.991	2.696	1.452	0.528	.....0.242
N39	4.003	1.577	1.047	1.177	1.042	0.538	0.171	.....0.082
N40	2.082	0.747	0.378	0.417	0.354	0.162	0.044	.....0.027

Table 4.6 Continues

N41	0.975	0.325	0.124	0.125	0.104	0.042	0.007	.....0.008
N42	0.421	0.135	0.037	0.029	0.024	0.011	0	.....0.002
N43	0.148	0.048	0.01	0.005	0.005	0.004	0	.....0.002
N44	0.036	0.013	0.003	0.001	0.001	0.002	0.001	.....0.002
N45	0.007	0.002	0.001	0	0	0.002	0.001	.....0.002
N46	0.001	0.001	0.001	0	0	0.001	0	.....0.002
N47	0	0	0	0	0	0	0	.....0.001
N48	0	0	0	0	0	0	0	.....0.001
N49	0	0	0	0	0	0	0	.....0.001
Z	36.7	36.7	36.6	36.2	35.3	34.5	33.4	.....31.4
RR	15.62	18.62	17.65	15.37	11.81	11.15	10.29	.....7.91
LWC	0.96	1.2	1.12	1.01	0.85	0.87	0.73	.....0.64
W	5.53	5.35	5.42	5.58	5.66	5.53	5.17	.....4.89